# MODULATION OF HOST ACTIN CYTOSKELETON BY A LEGIONELLA PNEUMOPHILA EFFECTOR

by

**Yao Liu**

**A Dissertation**

*Submitted to the Faculty of Purdue University*

*In Partial Fulfillment of the Requirements for the degree of*

**Doctor of Philosophy**


Department of Biological Sciences

West Lafayette, Indiana

December 2018

# THE PURDUE UNIVERSITY GRADUATE SCHOOL
# STATEMENT OF COMMITTEE APPROVAL

Dr. Zhao-Qing Luo, Chair
Department of Biological Sciences
Dr. Peter Hollenbeck
Department of Biological Sciences
Dr. Daoguo Zhou
Department of Biological Sciences
Dr. Seema Mattoo
Department of Biological Sciences

**Approved by:**

Dr. Stephen Konieczny
Head of the Graduate Program

*To my parents Shiling Liu and Haiyan Huang*
*my wife Wenqing Zhou and my daughter Grace Liu*

# ACKNOWLEDGMENTS

I would like to thank my wonderful supervisor Dr. Zhao-Qing Luo for his guidance throughout my PhD study. He is a very passionate and persevering scientist. When encountering an obstacle in the research, he would dwell in the problem day after day, until it was solved. Once he told us that he came up with an idea when he was taking a shower, which finally turned out to be a turning point of that project. His passion in science greatly influences me to pursue an academic career. He is also a very knowledgeable and inspiring supervisor. I really enjoy the time he shared with us seminal findings in the field during lab meetings. He not only talked about the discovery itself, but also the exciting story behind the discovery, which inspired us to be more creative in thinking, more thoughtful in designing experiments and more careful in analyzing results. Besides, he really cares the career development of his students. I still remembered when I first joined the lab, he read papers together with me every week for several months until I felt comfortable with the studies in the field. During the past five and a half years, no matter how busy he was, he would revise all my writings (thesis, manuscript, committee meeting reports, fellowship applications *et. al*) word by word and explain the reason to me to help me improve. He also gave me many invaluable suggestions during my postdoc lab searching and even recommended me to a PI who I am very interested in during an international conference. I am very fortunate to be a student of him.

I would like to thank my committee members Dr. Peter Hollenbeck, Dr. Daoguo Zhou and Dr. Seema Mattoo for their insightful suggestions and critical comments on my thesis projects. I would also like to thank Dr. Chris Staiger for generously sharing with us his equipment and helping us with actin-related assays. I thank Dr. Ernesto Nakayatsu at Pacific Northwest National Laboratory for his help in mass spectrometry. Last but not least, I would like to thank Dr. Qing Deng for her useful advices and great help.

I would like to dedicate my gratitude to my former labmate Dr. Wenhan Zhu, who is a great mentor. I literally learned every lab technique from him when I started in Dr. Luo's lab. His hardworking attitude, deep understanding of literature, and great presentation skills greatly influenced me in my earlier years and prompted me to improve myself from all aspects. I would like to thank our awesome former postdoctoral associate Dr. Jiazhang Qiu, who also shared with me a lot of useful techniques. He is very good at doing some "tricky" experiments such as growth

curve and immunostaining of infected amoebae cells, and always willing to share with me his experience. Ninghai Gan is a warmhearted person, who helped me a lot both inside and outside of the lab. I would also like to thank Victor Roman, Alix McCloskey, Dr. Canhua Lu, Dr. Xiaowen Fei, Jiayi Sun,Yan Liu, Kayla Perri, Jiaqi Fu and Chuang Li for sharing reagents and/or offering me help in the past a few years.

Finally, I would like to express my sincere gratitude to my parents for their selfless devotion and constant encouragements, to my wife for her love, understanding and tremendous support and to my daughter for bringing so much laughter and joy into my life.

# TABLE OF CONTENTS

# NOTE

**Chapters 1, 2 and 3 of the dissertation contain content of the following published unit:**

1. Liu Y, Zhu W, Tan Y, Nakayasu ES, Staiger CJ, Luo ZQ. A Legionella effector disrupts host cytoskeletal structure by cleaving actin. PLoS pathogens. 2017 Jan 27;13(1):e1006186.

# LIST OF FIGURES

# ABSTRACT

Author: Liu, Yao. PhD
Institution: Purdue University
Degree Received: December 2018
Title: Modulation of Host Actin Cytoskeleton by a *Legionella pneumophila* Effector.
Major Professor: Zhao-Qing Luo

*Legionella pneumophila*, the etiological agent of Legionnaires' disease, replicates intracellularly in protozoan and human hosts. Successful colonization and replication of this pathogen in host cells requires the Dot/Icm type IVB secretion system, which translocates over 330 effector proteins into the host cell to modulate various cellular processes. In this study, we identified RavK (Lpg0969) as a Dot/Icm substrate that targets the host cytoskeleton and reduces actin filament abundance in mammalian cells upon ectopic expression. RavK harbors an $H_{95}E_{XX}H_{99}$ (x, any amino acid) motif associated with diverse metalloproteases, which is essential for the inhibition of yeast growth and for the induction of cell rounding in HEK293T cells. We demonstrate that the actin is the cellular target of RavK and that this effector cleaves actin at a site between residues Thr351 and Phe352. Importantly, RavK-mediated actin cleavage occurs during *L. pneumophila* infection. Cleavage by RavK abolishes the ability of actin to form polymers. Furthermore, an F352A mutation renders actin resistant to RavK-mediated cleavage; expression of the mutant in mammalian cells suppresses the cell rounding phenotype caused by RavK, further establishing that actin is the physiological substrate of RavK. Thus, *L. pneumophila* exploits components of the host cytoskeleton by multiple effectors with distinct mechanisms, highlighting the importance of modulating cellular processes governed by the actin cytoskeleton in the intracellular life cycle of this pathogen.

# CHAPTER 1. INTRODUCTION

## *Legionella pneumophila* and Dot/Icm Type IV secretion system

*Legionella pneumophila,* the etiological agent of Legionnaires' disease, is a Gram-negative, opportunistic bacterial pathogen. It is ubiquitously found in the aquatic environments, and mainly survives within a broad range of amoebae hosts, but free-living or biofilm-associated bacteria have also been reported (Lau & Ashbolt, 2009). It becomes a health threat to human beings once it thrives in man-made water systems such as air conditioning cooling towers. The inhalation of small water droplets containing *L. pneumophila* by immunocompromised individuals can lead to either a potentially fatal Legionnaires' disease or a mild flu-like illness called Pontiac fever (Newton, Ang et al., 2010).

The first known outbreak of Legionnaires' disease occurred during the American Legion convention on July 21$^{st}$, 1976 at the Bellevue-Stratford hotel in Philadelphia. In this outbreak, 182 people were reported to contract a pneumonia-like disease, and unfortunately 29 people died due to pneumonia-like symptoms. The causative agent of this outbreak remained mysterious for approximately half a year until Dr. Joseph McDade identified the bacterium and subsequently named it as *Legionella pneumophila* (McDade, Shepard et al., 1977). For a long time, replication in human cells is considered as a dead end for *L. pneumophila*, because few human-to-human transmissions were reported even for large-scale outbreaks (Fraser, Tsai et al., 1977). But recently, a probable human-to-human transmission case was reported in Portugal (Correia, Ferreira et al., 2016). The cases of Legionnaires' disease in the United States has been on the rise since 2000, and in 2016 over 6100 cases were reported to Centers for Disease Control and Prevention. (Prevention., 2017). However, since Legionnaires' disease can be easily underdiagnosed, the actual cases could be much more.

To survive within amoebae hosts as well as human alveolar macrophages, *L. pneumophila* has evolved an arsenal of weapons to subvert host anti-microbial defenses. After being engulfed by phagocytes such as amoebae and macrophages, *L. pneumophila* colonizes a membrane-bound organelle, which is often referred to as *Legionella*-containing vacuole (LCV). By hijacking host membrane trafficking pathways, the LCV membranes are quickly converted from nascent phagosome-like membranes to rough endoplasmic reticulum (ER)-like membranes, which

prevents the LCV from proceeding to the phagosome maturation process for destruction. Shielded by the LCV from host cytoplasmic defense, *L. pneumophila* replicates to large numbers, egresses the vacuole, lyses the cell to infect neighboring cells to start a new round of intracellular cycle (**Fig. 1-1**) (Isberg, O'Connor et al., 2009).

Although the causative agent of Legionnaires' disease was identified in 1977, virulence factors of *L. pneumophila* were not discovered until early 1990s. The attempt to identify *L. pneumophila* virulence factors required for intracellular multiplication became possible after Shuman and colleagues isolated mutants from strain Philadelphia 1 with enhanced ability to serve as a heterospecific mating recipient (Marra & Shuman, 1989). By serial passage of wild-type *L. pneumophila* on suboptimal medium, Horwitz identified 44 avirulent mutants which had lost the ability to replicate intracellularly (Horwitz, 1987). Shuman and colleagues obtained one of the avirulent mutants 25D, and isolated a fragment of genome DNA able to restore the intracellular growth defect of 25D, which was designated as the *icm* region (for intracellular multiplication) (Marra, Blander et al., 1992), Two years later, the *icm* region was shown to contain four open reading frames *icmW*, *icmX*, *icmY* and *icmZ* (Brand, Sadosky et al., 1994).

At almost the same time, Berger and Isberg used an exquisite intracellular thymineless enrichment strategy to isolate a few mutants defective in both intracellular replication and organelle trafficking, and identified the *dot* locus (for defect in organelle trafficking) that can complement both phenotypes induced by the mutants in macrophages (Berger & Isberg, 1993). One year later, they found that the *dotA* gene alone within the *dot* locus is able to restore the phenotypes of the mutants (Berger, Merriam et al., 1994).

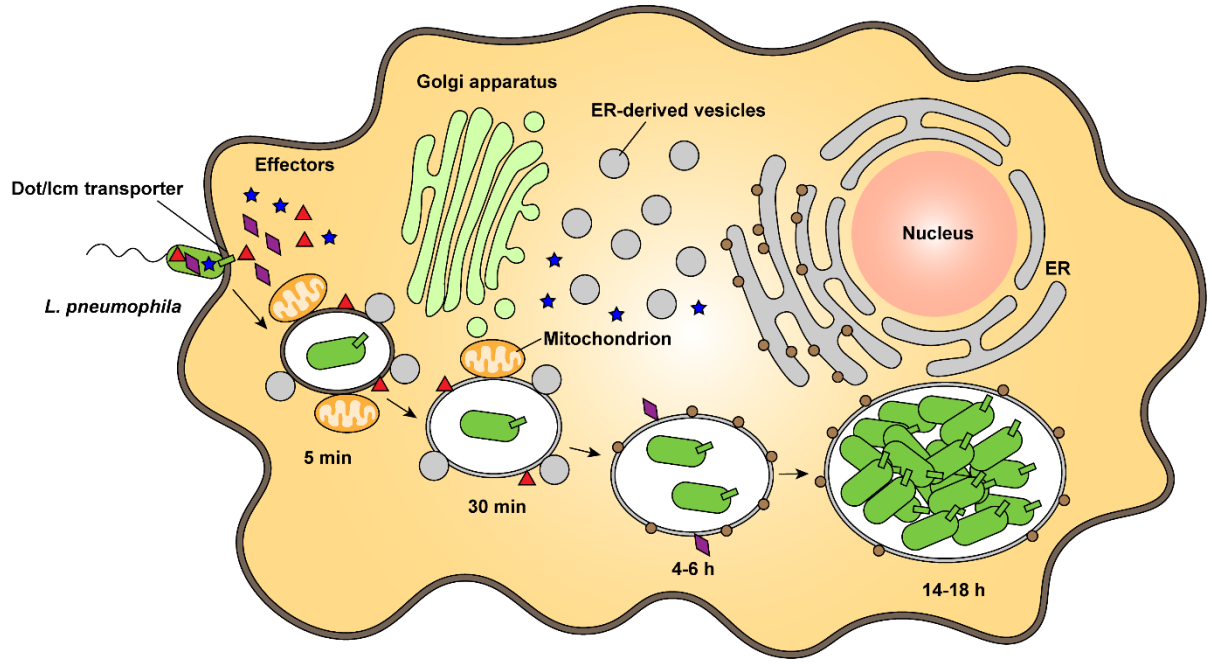


**Fig. 1-1 *L. pneumophila* modulates host trafficking pathway to establish a vacuole permissive for its replication.**

After being engulfed by host cell via phagocytosis, the *Legionella*-containing vacuole (LCV) can evade host endocytic pathway and actively recruit ER-derived vesicles and mitochondria. As a consequence, the plasma-membrane-derived phagosomal membrane is rapidly transformed into ER-like membrane, and in the later phase of infection becomes studded by ribosomes. Inside the vacuole, *L. pneumophila* replicates to high numbers and eventually lyses the cell to infect neighboring cells. The whole process strictly requires the Dot/Icm type IV secretion system, through which more than 330 effector proteins are translocated into host cell.

Since there is a correlation between a strain's ability to kill host cells and its virulence in guinea pig (Fields, Barbaree et al., 1986, Marra et al., 1992, Pearlman, Jiwa et al., 1988), The Shuman lab isolated 55 Tn903dIIlacZ transposon mutants defective in macrophage killing and mapped the mutated genes in those mutants (Purcell & Shuman, 1998, Sadosky, Wiater et al., 1993, Segal, Purcell et al., 1998, Segal & Shuman, 1997). Meanwhile, the Isberg lab isolated 6 mutants induced by ethyl methanesulfonate, which are defective in macrophage killing; they subsequently mapped the loci carrying these mutations in each mutant (Merriam, Mathur et al., 1997). In addition, inspired by the observation that salt resistance and the ability to kill host cells are phenotypically relevant (i.e. mutants resistant to salts are also defective in intracellular replication), the Isberg lab used salt to isolate *L. pneumophila* mutants defective in intracellular replication (Vogel, Roy et al., 1996). Taken together, by 1998, 23 *dot*/*icm* genes located at two separated regions in the *L. pneumophila* genome have been identified by the two groups (Segal & Shuman, 1998).

Interestingly, among the 23 proteins encoded by loci of the *dot/icm* regions, five of them (DotB, DotG, DotI, DotL and DotM) share limited sequence similarity to plasmid-encoded proteins involved in conjugal DNA transfer (Vogel, Andrews et al., 1998, Vogel et al., 1996), which prompts both Isberg's group and Shuman's group to test whether Dot/Icm proteins can mediate DNA transfer between bacteria. Indeed, the products of *dot*/*icm* genes assemble into a functional DNA conjugation system which allows the transfer of mobilizable but not self-conjugal IncQ plasmids from one cell to another (Segal et al., 1998, Vogel et al., 1998). After the sequences of IncI plasmids *col*Ib-P9 and R64 became available in 1999, it was clear that *dot*/*icm* genes are closely related to *tra*/*trb* genes from members of the IncI plasmid group (Komano, Yoshida et al., 2000, Segal & Shuman, 1999, Wilkins & Thomas, 2000). However, DNA is unlikely the primary substrates of the Dot/Icm protein complex because prevention of phagosome-lysosome fusion occurs as early as 5 minutes after bacterial uptake, which is probably not enough for bacterial DNA to be transferred, transcribed and translated in the host. (Roy, Berger et al., 1998). In agreement with this prediction, the first protein substrate of the Dot/Icm system RalF was identified in 2002 by its high-level similarity to Sec7 domains found in guanine nucleotide exchange factors (GEF) of the Arf family small GTPases, which established that the Dot/Icm system can translocate effector proteins into host cells (Nagai, Kagan et al., 2002). So far, 27 Dot/Icm proteins have been identified, which are believed to assemble into a protein complex spanning bacterial inner

membrane, outer membrane and host phagosomal membrane (Isberg et al., 2009). Due to its limited similarity to the original Type IV secretion system identified in *Agrobacterium tumefaciens*, the Dot/Icm secretion system is classified as a Type IVB secretion system (Nagai & Kubori, 2011).

After the identification of the components of the Dot/Icm secretion system for more than 20 years, recent studies have begun to reveal how those proteins assemble into a functional Type IV secretion system. In 2014, Nagai and his colleagues visualized the native Dot/Icm transporter as a ring-shaped structure using transmission electron microscopy. They also isolated the Dot/Icm core complex using a biochemical method. The core complex consists of at least five proteins: DotC, DotD, DotH, DotF and DotG. DotC and DotD are lipoproteins localized to bacterial outer membrane. DotH is an outer-membrane associated protein, whose localization to membrane requires DotC and DotD. DotG forms a channel spanning inner-membrane and outer-membrane and is essential for translocation of Dot/Icm substrates into host cytosol. DotF, in contrast, is dispensable for effector translocation but it facilitates the assembly of DotG into DotC-DotG-DotH complex (Kubori, Koike et al., 2014). In 2015, the structure of DotI, an inner membrane protein essential for effector translocation, was solved. The structure of DotI resembles that of VirB8 from Type IVA secretion systems despite of a very low similarity between their primary sequences. DotI forms a stable complex with DotJ. The DotI-DotJ complex does not stably interact with the five-protein core complex described above, so how DotI facilitates effector translocation remains enigmatic (Kuroda, Kubori et al., 2015).

In 2017, Jensen's group used electron cryotomography (ECT) to visualize the structure of Dot/Icm transporter in *L. pneumophila* cells. They found that the overall structure of Dot/Icm transporter shares a significant similarity with that of a type IVA secretion system encoded by the R388 plasmid in *E. coli*, although the structure of Dot/Icm complex is longer and wider (Ghosal, Chang et al., 2017).

In the same year, Oh's group determined the structure of the type IV coupling protein (T4CP) complex, which links translocating effectors to secretion channel. The Dot/Icm T4CP is made up of at least five proteins: DotL, DotN, IcmS, IcmW and LvgA. IcmS-IcmW protein complex was shown to mediate the translocation of a subset of Dot/Icm substrates (Cambronne & Roy, 2007, Ninio, Zuckman-Cholon et al., 2005). DotL is a hexameric ATPase, harboring an ATPase domain and a C-terminal extension domain. The C-terminal domain of DotL interacts with

the other four proteins, forming a substrate-recognition domain that directly binds Dot/Icm substrates (Kwak, Kim et al., 2017). The structures of a portion of T4CP complex consisting of IcmS, IcmW and DotL was solved recently. The structures showed that IcmS/IcmW complex uses the same hydrophobic region that binds effectors to interact with DotL (Xu, Xu et al., 2017). DotM is a transmembrane protein, which interacts with DotL and DotN to form the coupling complex. In 2018, Waksman's group solved the structure of DotM. They found that the structure of DotM contains multiple patches of positively charged residues, which are essential to bind a class of effectors containing E-block sequences (Huang, Boyd et al., 2011). Importantly, *L. pneumophila* strains expressing DotM mutants lacking these patches is defective in the translocation of E-block-containing effectors via the Dot/Icm transporter (Meir, Chetrit et al., 2018).

Recently, Liu's group and Roy's group found that the ATPase DotB is associated with the core complex of the Dot/Icm transporter by interacting with DotO, another ATPase. They further solved the structure of the DotB-DotO ATPases complex in situ by cryo-electron tomography. The structure reveals that a hexamer of DotO dimers directly interacts with the inner membrane complex, and a hexamer of DotB attaches to the base of the cytoplasmic complex. DotB and DotO together creates a cytoplasmic channel important for the translocation of effectors via the Dot/Icm transporter (Chetrit, Hu et al., 2018).

Notably, the localization of the Dot/Icm transporter is also essential for the virulence of *L. pneumophila*. The Dot/Icm transporter localizes to bacterial poles and polar translocation of effectors appears to be critical for virulence, because similar efficiency of effector translocation from non-polar regions does not support intracellular bacterial growth (Jeong, Ghosal et al., 2017).

## Protein substrates of Dot/Icm secretion system

Since the identification of the first effector protein in 2002, more than 330 effector proteins have been identified so far by a diverse array of methods (Qiu & Luo, 2017). These effectors were generally identified by the following six methods. First of all, bioinformatics analyses were used to identify *L. pneumophila* proteins that harbor eukaryotic-like motifs, which likely play a role in the host cell (Chen, de Felipe et al., 2004, de Felipe, Pampou et al., 2005, Nagai et al., 2002, Pan, Luhrmann et al., 2008). Secondly, a number of effector proteins were identified by their interactions with different Dot/Icm proteins, such as DotF (Luo & Isberg, 2004), IcmS (Bardill, Miller et al., 2005) and IcmW (Ninio et al., 2005). The study by Luo and Isberg first revealed the

potential functional redundancy among effectors as mutants lack a single effector gene rarely display detectable defects in intracellular growth in commonly used infection models (Luo & Isberg, 2004). Thirdly, common features of signal sequence for translocation such as E-block motif were deduced from known *L. pneumophila* effectors, and were used as a proxy for predicting new effectors, which allows the identification of a lot more effectors (Burstein, Zusman et al., 2009, Huang et al., 2011, Lifshitz, Burstein et al., 2013, Nagai, Cambronne et al., 2005). Fourthly, the expression of many known effectors was found to be regulated by regulators such as PmrA and CpxR, therefore novel effector coding genes were identified by using the consensus regulatory sequences recognized by PmrA or CpxR (Altman & Segal, 2008, Zusman, Aloni et al., 2007, Zusman, Degtyar et al., 2008). Fifthly, ectopic expression of many *L. pneumophila* effectors in yeast was shown to interfere with cellular pathways or even arrest yeast growth, therefore screenings of *L. pneumophila* proteins that disrupt yeast cellular pathways were also used to identify effector proteins (Campodonico, Chesnel et al., 2005, Heidtman, Chen et al., 2009, Shohdy, Efe et al., 2005). Lastly, a large proportion of effector proteins were identified by direct screening of *L. pneumophila* proteins that can be translocated into host cells (Huang et al., 2011, Zhu, Banga et al., 2011b). It is worth mentioning that candidates identified by method 1-5 have to be validated by translocation assays such as interbacterial protein transfer, immunofluorescence staining with SidC-specific antibody (Huang et al., 2011, Luo & Isberg, 2004), Cya-fusion assay and the β-lactamase-based Assay (Zhu & Luo, 2013).

## Modulation of host cellular pathways by *L. pneumophila*

### Modulation of endocytic pathway

After phagocytosis by amoebae hosts or human alveolar macrophages, non-pathogenic microorganisms reside in nascent phagosomes, which sequentially interact with early endosomes, late endosomes and lysosomes, and finally being degraded in acidic phagolysosome. The LCV, however, can deviate from the default endocytic pathway as early as 5 minutes post-infection, which requires the Dot/Icm secretion system (Roy et al., 1998). Besides, it rapidly recruits ER-derived vesicles and mitochondria. Eventually, the plasma membrane-derived LCV membrane is converted to rough ER-like membrane (Tilney, Harb et al., 2001).

The modulation of endocytic pathways by *L. pneumophila* is achieved by various effectors via different mechanisms. The four main strategies used by *L. pneumophila* are: the hijacking of

small GTPases involved in endocytic trafficking, the modulation of the phosphatidylinositol (PI) lipids composition on the endosomal membrane, the modulation of vacuolar ATPase (V-ATPase) to fine-tune luminal pH and the inhibition of the function of retromer.

***Hijacking of small GTPases in endocytic trafficking***

Rab35 is a small GTPase involved in the sorting of cargos from early endosomes, and the inactivation of Rab35 leads to the enlargement of early endosome (Allaire, Marat et al., 2010). A *L. pneumophila* effector AnkX has been shown to inactivate this small GTPase by phosphocholination to inhibit the endocytic trafficking (Mukherjee, Liu et al., 2011).

Lpg0393 was identified as a guanine-nucleotide exchange factor (GEF) for endosomal small GTPases Rab5, Rab21 and Rab22 due to its structural similarity to Rabex-5, a GEF for Rab5 (Sohn, Shin et al., 2015). But its significance during *L. pneumophila* infection was not explored further.

***Modulation of PI composition on the endosomal membrane***

Rab5 is an early endosome-localized small GTPase. The effector proteins of active Rab5 includes EEA1 and hVps34. hVps34 is a PI 3-kinase, which generates PI(3)P, a signature phospholipid of early endosome. EEA1 is a tethering protein on the surface of early endosome by binding to PI3P, which is required for the fusion of vesicles with early endosome (Grosshans, Ortiz et al., 2006). *L. pneumophila* specifically disrupts the early endosome function by secreting an effector VipD, which exhibits phospholipase A1 activity against PI(3)P in the presence of Rab5 or a similar endosomal small GTPase Rab22. The depletion of PI3P from endosomal membrane by VipD renders the endosomes fusion incompetent, therefore deviates the LCV from endocytic pathway (Gaspar & Machner, 2014, Ku, Lee et al., 2012).

***Modulation of vacuolar pH by targeting V-ATPase***

The maturation of the phagosome is accompanying with a decreasing pH of phagosome. The early endosome is mildly acidic with a pH around 6.1; the late endosome has pH between 5.5-6.0; and the lysosome often has a luminal pH between 4.5-5.5 (Scott, Botelho et al., 2003). In the early phase of infection (3-6 h post infection), the average pH of phagosomes containing live *L. pneumophila* is 7.4, comparing to 5.5 in those containing heat-killed *L. pneumophila*. But in the late phase (16-22 h post infection), the average pH of the LCV is 5.5, which is similar to the pH

of late endosome/lysosome (Sturgill-Koszycki & Swanson, 2000). These results suggest that *L. pneumophila* modulates the pH of the LCV in the early phase of infection. In consistent with this, a *L. pneumophila* effector SidK was found to inhibit the acidification of the LCV in the early phase of infection by binding to and inhibiting the activity of vacuolar ATPase. (Xu, Shen et al., 2010b).

***Inhibition of the function of retromer***

Retrograde trafficking is the process to transport cargoes from endosome exit site to the trans-Golgi network (TGN). Retromer, a five-subunit protein complex, is essential for the process (Bonifacino & Hurley, 2008). A *L. pneumophila* effector RidL inhibits retrograde trafficking by directly interacting with Vps29, a subunit of the retromer complex (Finsel, Ragaz et al., 2013). The molecular mechanism of the inhibition of retrograde trafficking by RidL was independently revealed by three groups recently. All the studies suggest that RidL outcompetes an important regulator of retromer TBC1d5 for the same binding site on Vps29, thereby inhibiting retromer activity (Barlocher, Hutter et al., 2017, Romano-Moreno, Rojas et al., 2017, Yao, Yang et al., 2018).

**Modulation of secretory pathway**

The secretory pathway transports cargoes from the ER to the Golgi apparatus and finally to their target organelles. Vesicles that mediate cargo transport between different organelles generally are formed by different coating proteins. For example, trafficking from the ER to the Golgi apparatus is mediated by vesicles formed by coating protein COPII; vesicles leaving Golgi for downstream organelles are coated with clathrin; vesicles that traffick from the Golgi back to the ER are coated with COPI.

Members of Ras superfamily GTPases are important regulators of vesicle trafficking pathways including the secretory pathway. These regulatory small GTPases oscillate between active and inactive forms depending on their nucleotide-binding status. GTP-binding allows them to assume an active conformation, thus interacting with their downstream effector proteins. In contrast, binding to GDP (caused by GTP hydrolysis) renders them inactive. The majority of small GTPases contain a hydrophobic tail. In the case of Rab family small GTPases, when in the inactive form, they are sequestered by guanine nucleotide dissociation inhibitors (GDIs) in the cytosol. When proper signals are received, the GDI displacement factors (GDFs) trigger the dissociation

of GDIs and GDP-bound small GTPases, exposing their hydrophobic tails. The exposed hydrophobic tails mediate the targeting of small GTPases to membrane, where they can be activated by guanine nucleotide exchange factors (GEFs) to the GTP-bound form. Finally, the GTP-bound small GTPases are inactivated by guanine nucleotide activating proteins (GAPs) to the GDP-bound form, which can be extracted by GDIs from membrane and sequestered in the cytosol. For Sar/Arf family small GTPases, GDIs are not involved. Instead, they are released from membranes following GTP hydrolysis that induces a structural change rendering their hydrophobic tails being masked (Mizuno-Yamasaki, Rivera-Molina et al., 2012).

The Sar1 small GTPase is essential for the budding of COPII-coated vesicles from the ER, Arf1 is responsible for the budding of COPI-coated or clathrin-coated vesicles from the Golgi apparatus or plasma membrane, and Rab family small GTPases are key players in the transport of vesicles through the cytoskeletal structures, tethering and fusion of vesicles with recipient compartments (Mizuno-Yamasaki et al., 2012).

It has been known for more than twenty years that the LCV is enriched with ER resident proteins (Swanson & Isberg, 1995). In 2002, Roy and colleagues revealed that *L. pneumophila* intercepts ER-derived vesicles from the ER exit site by using inhibitors targeting different steps of vesicle trafficking. They also found that small GTPases Sar1 and Arf1 are important for the biogenesis of the LCV (Kagan & Roy, 2002a). In the same year, the first *L. pneumophila* Dot/Icm effector RalF was identified, which functions as a GEF for the small GTPase Arf1 and is responsible for the recruitment of Arf1 to the LCV (Nagai et al., 2002).

In 2004, Rab1 and Sec22b were shown to be associated with the LCV (Derre & Isberg, 2004, Kagan, Stein et al., 2004). In 2006, two groups independently identified that SidM, also known as DrrA, is a GEF for Rab1 and is responsible for the recruitment of Rab1 to the LCV (Machner & Isberg, 2006, Murata, Delprato et al., 2006). One year later, both groups further showed that SidM also serves as a GDF to dissociate Rab1 from GDI (Ingmundson, Delprato et al., 2007, Machner & Isberg, 2007). In the same study, Roy's group also identified that *L. pneumophila a* type IV effector LepB is a GAP for Rab1, which catalyzes the conversion of GTP-Rab1 to GDP-Rab1 (Ingmundson et al., 2007). A study based on the structure of the N-terminal domain of SidM revealed that SidM catalyzes the transfer of adenosine monophosphate from adenosine triphosphate (ATP) to the Tyrosine-77 of Rab1, therefore blocking its interaction with LepB (Muller, Peters et al., 2010). In 2011, two groups independently identified a *L. pneumophila*

effector SidD that can remove the AMP moiety from Rab1, thereby allowing the hydrolysis of Rab1 catalyzed by LepB (Neunuebel, Chen et al., 2011, Tan & Luo, 2011b). What further complicates Rab1 modulation by *L. pneumophila* is the discovery of AnkX and Lem3 (Mukherjee et al., 2011, Tan & Luo, 2011b). AnkX is a Fic-domain containing protein, which modifies Rab1 at Serine-76 by phosphorylcholination, thus interfering with its activation, GTP hydrolysis catalyzed by GAPs such as LepB as well as its interaction with GDI; while Lem3 functions to remove the phosphorylcholine group from Rab1 (Goody, Heller et al., 2012, Oesterlin, Goody et al., 2012, Tan, Arnold et al., 2011). Ubiquitination of Rab1 was also reported. E3-ubiquitin ligases SidC and SdcA is associated with the mono-ubiquitination of Rab1 during infection, but whether SidC/SdcA directly catalyzes the ubiquitination reaction remains to be determined (Horenkamp, Mukherjee et al., 2014). In addition, mono-ubiquitination of Rab1 catalyzed by the SidE family proteins was also reported, but how this modification affects the Rab1 function remains elusive (Qiu, Sheedlo et al., 2016).

SNARE [soluble N-ethylmaleimide-sensitive factor (NSF) attachment protein receptor] proteins are a family of proteins that directly mediate the fusion between vesicles and their target membrane bound organelles. SNARE proteins can be divided into four subfamilies, Qa-, Qb, Qc- and R-SNAREs, and one from each subfamily is required for the assembly of a functional SNARE complex (Fasshauer, Sutton et al., 1998). Due to their essential roles in vesicle trafficking, it's not surprising that *L. pneumophila* has evolved different strategies to target SNAREs.

In 2010, Roy and colleagues found that Sec22b, an R-SNARE involved in the trafficking between the ER and the Golgi apparatus, can form noncanonical pairing with plasma membrane (PM)-localized Q-SNAREs (Syntaxin2, 3, 4 and SNAP-23) during *L. pneumophila* infection, which allows Sec22b to be associated with the LCV membranes derived from the PMs. Furthermore, the noncanonical pairing of SNAREs is important for the fusion of the LCV with ER-derived vesicles and requires an intact Dot/Icm secretion system (Arasaki & Roy, 2010). Two years later, the multifunctional *L. pneumophila* effector SidM was found to activate Rab1 on the LCV to stimulate the pairing between Sec22b and PM-localized SNAREs, promoting the fusion between the LCV and ER-derived vesicles (Arasaki, Toomre et al., 2012). Recently, Arasaki's group and Roy's group co-discovered that the SidM-stimulated recruitment of ER-derived vesicles to the LCV requires Sec5 and Sec15, two subunits of exocyst, which function in the tethering of ER-derived vesicles to PM-derived the LCV (Arasaki, Kimura et al., 2018).

Mimicry of host SNAREs by *L. pneumophila* was another commonly used strategy to hijack host vesicle trafficking. The effector LseA was identified as a homolog of Qc-subfamily SNARE in a bioinformatic screen. In mammalian cells, farnesylated LseA localizes to the Golgi apparatus and interacts with a subset of Qa, Qb and R-SNAREs, but whether and how such modulation impacts host trafficking pathway during infection remains unknown (King, Newton et al., 2015). The LegC family effectors (LegC2, LegC3 and LegC7) were identified as homologs of Q-SNAREs also by a bioinformatics method. During infection, the three effectors specifically form a complex with host R-SNARE VAMP4, a protein involved in trans-Golgi network vesicle trafficking. Interestingly, the complex formed by LegC proteins and VAMP4 cannot be disassembled by N-ethylmaleimide-sensitive factor, therefore *L. pneumophila* can continuously recruit VAMP4-containing vesicles for the expansion of the LCV, and trapping VAMP4 in its inactive form (Shi, Halder et al., 2016).

**Modulation of the host ubiquitin system**

Ubiquitination is an essential post-translational modification that is implicated in many cellular processes such as protein degradation by proteasome, DNA repair, cell cycle progression and numerous signal transduction pathways (Kerscher, Felberbaum et al., 2006). Generally, ubiquitination requires a cascade of three enzymes Ubiquitin (Ub)-activating enzyme E1, Ub-conjugating enzyme E2 and E3 Ub ligase to catalyze the formation of an isopeptide bond between the carboxyl group of C-terminal Gly of Ub and the ε-amino group of a Lys in the substrate. Although Ub is not present in prokaryotes, many bacterial symbionts and pathogens, including *L. pneumophila* have evolved various strategies to hijack this pathway for their own benefits.

The first evidence of the modulation of host ubiquitin cascades by *L. pneumophila* came from the finding that the LCV are decorated with polyubiquitin conjugates in a Dot/Icm dependent manner (Dorer, Kirton et al., 2006). Consistent with this observation, so far more than 10 *L. pneumophila* effectors have been shown to modulate host ubiquitin system by various mechanisms. Most of these effectors target Ub system by mimicking host E3 Ubiquitin ligases. At least 6 F-box containing-, and 2 U-box containing effectors have been identified *in silico* (Hubber, Kubori et al., 2014b). LegU1 is an F-box-containing effector, which is able to ubiquitinate BAT3 *in vitro* and possibly to modulate apoptosis or host ER stress response (Ensminger & Isberg, 2010). LubX is a U-box containing effector, which catalyzes the ubiquitination of a host cell cycle-related

kinase Clk1 and a *L. pneumophila* effector SidH (Kubori, Hyakutake et al., 2008, Kubori, Shinzawa et al., 2010). The poly-ubiquitination of SidH targets it to proteasome for degradation. Interestingly, the translocation of LubX into host cell is not detectable until 8 hours post infection, which allows the SidH to play its function only in the early phase of infection, highlighting a mechanism of temporal regulation of one effector's activity by another effector (Kubori et al., 2010). The E3 ligase activity of another U-Box-containing effector GobX was also experimentally confirmed, but its substrates remain elusive (Lin, Doms et al., 2015). Recently, five *L. pneumophila* effectors (RavN, Lpg2530, Lpg2577, Lpg2498 and Lpg2452) which bare limited primary sequence similarities to classical E3 ligases were identified by protein pulldown or a secondary structure-based prediction method and experimentally verified as novel E3 ligases (Lin, Lucas et al., 2018). Besides, *L. pneumophila* also encodes a family of novel Ub E3 ligases (SidC and SdcA), which adapt a Cys-His-Asp triad commonly present in cysteine proteases for catalyzing ubiquitination. Importantly, the E3 ligase activity is essential for the SidC-mediated recruitment of ER proteins and polyubiquitin-conjugates to the LCV (Hsu, Luo et al., 2014).

Ubiquitination is reversible. The removal of Ub from substrates or other molecules is achieved by deubiquitinases (DUBs). In *L. pneumophila*, at least five effectors have been shown to possess a DUB activity. Four members of SidE family (SidE, SdeA, SdeB, SdeC) each harbor a DUB domain on its N-terminus, which cleaves Lys11-, Ly48, Ly63-linked di-Ub, with a preference toward Lys63-linked Di-Ub. The DUB activity of SidE members is not necessary for proficient intracellular replication of *L. pneumophila* in different hosts, but is required for the dynamics of the association of poly-ubiquitin conjugates with the LCV (Sheedlo, Qiu et al., 2015). LotA was identified as a DUB due to its limited sequence similarity to eukaryotic ovarian tumor (OTU) family DUBs. During infection, LotA localizes to the LCV by binding to PI(3)P, and also plays a role in regulating the association of ubiquitinated protein species with the LCV (Kubori, Kitao et al., 2018).

The most exciting finding in the *Legionella* field may be the recent discovery of a family of non-canonical Ub ligases (Qiu et al., 2016). Members of SidE family catalyze the ubiquitination of multiple small GTPases involved in the ER to the Golgi trafficking as well as the ER protein reticulon 4 (RTN4) by a mechanism independent of E1 and E2 enzymes (Kotewicz, Ramabhadran et al., 2017, Qiu et al., 2016). The ubiquitination is achieved first by a mono-ADP-ribosyl transferase (mART) domain that activates Ub by ADP-ribosylation at residue Arg42 to form ADP-

ribosylated Ub (ADPR-Ub) (Qiu et al., 2016). In the subsequent reaction, a phosphodiesterase (PDE) domain also embedded in the same proteins converts the ADPR-Ub to phosphoribosylated Ub (Bhogaraju, Kalayil et al., 2016, Kotewicz et al., 2017). Concomitantly, Phosphoribosylated Ub is linked to serine residues on substrates or SdeA itself accompanied by the release of AMP (Bhogaraju et al., 2016). Importantly, both the mART domain and the PDE domain are required for proficient intracellular replication of *L. pneumophila* in its protozoan host (Kotewicz et al., 2017, Qiu et al., 2016). The ubiquitination of RTN4 catalyzed by SidE family proteins induces rearrangement of the ER tubules and recruitment of RTN4 on the LCV, but the biological significance of the RTN4 recruitment remains elusive (Kotewicz et al., 2017). Similarly, how the SidE family proteins-mediated-ubiquitination of small GTPases such as Rab33b promotes intracellular replication of *L. pneumophila* requires further investigation (Qiu et al., 2016).

**Modulation of host lipid metabolism**

Lipids play essential roles in the cell such as acting as components of cell membranes, energy storage, membrane trafficking and cell signaling, therefore it's not surprising that host lipid metabolism is a hotspot targeted by various *L. pneumophila* effectors. Phosphatidylinositides (PIs) are a group of lipids important for defining the signature of distinct organelles. Seven different PIs are present in the cell depending on their phosphorylation statuses of the 3', 4' 5' position of the inositol headgroup. Generally, different membrane-bound compartments have their specific PI profiles. For example, phosphatidylinositol 3,4,5-triphosphate [PI(3,4,5)P3] and phosphatidylinositol 4,5-biphosphate [PI(4,5)P2] are enriched in the PM, phosphatidylinositol 3-phosphate [PI(3)P] is enriched in endosomes and phosphatidylinositol 4-phosphate [PI(4)P] is enriched in the Golgi apparatus as well as the PM (Di Paolo & De Camilli, 2006).

PI(4)P has been shown to be enriched on the LCV membrane and at least five *L. pneumophila* effectors (SidC, SdcA, SidM, Lpg2603, Lpg1101) are localized to the LCV by specifically binding to this lipid species (Brombacher, Urwyler et al., 2009, Hubber, Arasaki et al., 2014a, Weber, Ragaz et al., 2006). The accumulation of PI(4)P on the LCV is regulated by a complex process involving various sources of PI(4)P as well as multiple kinases and phosphatases from both the host and the bacterium. PI(4)P can be derived from PI(3)P and/or PI(3,4,5)P3, because both lipids are enriched on the LCV membrane within 1 min post infection in a Dot/Icm-independent manner (Weber, Wagner et al., 2014). Besides, PI(3)P on the LCVs containing WT

*L. pneumophila* is slowly lost in the first 2 hours post infection, meanwhile PI(4)P gradually accumulates on these vacuoles (Weber et al., 2014). When PI(3)P is used as the source for PI(4)P, it is first converted to PI(3,4)P2 by LepB, a PI 4-kinase from *L. pneumophila* (Dong, Niu et al., 2016). As the *L. pneumophila* effector SidF possesses a PI 3-phosphatase activity toward both PI(3,4)P2 and PI(3,4,5)P3, the product of LepB - PI(3,4)P2 can be converted to PI4P by SidF (Hsu, Zhu et al., 2012). The fact that accumulation of PI(4)P on the LCVs containing Δ*lepB*Δ*sidF* is comparable to those containing Δ*lepB* or Δ*sidF* alone corroborates the notion that LepB and SidF act on the same pathway to generate PI(4)P (Dong et al., 2016). Alternatively, when PI(3,4,5)P3 is the source, it is first converted PI(4,5)P2 first by SidF. PI(4,5)P2 can be further converted to PI(4)P by the host PI 5-phosphatase OCRL1, which has been reported to be associated with the LCV in a Dot/Icm-dependent manner (Weber, Ragaz et al., 2009). Another mechanism to generate PI(4)P on the LCV is the phosphorylation of PI on its 4' position, indeed it was found that an ER-PM contact site localized PI 4-kinase - PI4KIIIα is required for optimal PI(4)P enrichment on the LCV as well as proficient intracellular growth of *L. pneumophila* in BMDMs (Hubber et al., 2014a).

*L. pneumophila* also encodes several effectors, whose functions contribute to lipid metabolism in infected cells but may not be directly linked to the accumulation of PI(4)P on the LCV. For example, SidP is a PI 3-phosphatase that can specifically dephosphorylate PI(3)P and PI(3,5)P2 to PI and PI(5)P respectively, but how SidP benefits the intracellular life cycle of *L. pneumophila* is elusive (Toulabi, Wu et al., 2013). VipD possesses a phospholipase A1 activity toward PI(3)P, and its role in endocytic pathway has been described above. Besides, *L. pneumophila* effector LpdA is a phospholipase D that converts phosphatidylcholine to phosphatidic acid, the latter can be further converted to diacylglycerol by another *L. pneumophila* effector LecE. As both LpdA and LecE localize to the LCV, their coordinate activities may result in the accumulation of diacylglycerol on the LCV, but how it would influence the intracellular growth of *L. pneumophila* has not been fully explored (Viner, Chetrit et al., 2012).

## Modulation of actin cytoskeleton

### *Hijacking host actin nucleator and actin-binding protein*

Arp2/3 complex, consisting of seven subunits, is an important actin nucleator that catalyze the branching of daughter filaments from existing filament at a distinctive 70 degree angle (Mullins

& Pollard, 1999). In 2015, Doublet's group showed that the type IV effector LegK2(Lpl2066) from *L. pneumophila* Paris strain phosphorylates the Arp3 and ArpC1B subunits of the Arp2/3 complex to inhibit actin polymerization around the LCV, which further prevents the association of the LCV with late endosome/lysosome network (Michard, Sperandio et al., 2015).

Profilin is an important actin-binding protein, which interacts with actin monomer at a 1:1 ratio and catalyzes the adenosine diphosphate (ADP) to ATP nucleotide exchange on actin monomers (Mockrin & Korn, 1980). In addition, profilin was found to promote formin-mediated filaments formation while inhibits Arp2/3 mediated-branch formation (Suarez, Carroll et al., 2015). Interestingly, it was found that yeast profilin specifically suppresses the yeast toxicity induced by the *L. pneumophila* type IV effector Ceg14. Furthermore, the actin-binding activity of profilin is required for the suppressor activity. Although Ceg14 does not detectably interact with profilin, it was shown to co-sediment with filamentous actin and inhibits actin polymerization *in vitro* with an unknown molecular mechanism (Guo, Stephenson et al., 2014b).

***Mimicking host actin nucleator***

VipA was first identified as a type IV effector that modulates the Multivesicular Body (MVB) pathway in a screening for *L. pneumophila* effectors capable of interfering with vesicle trafficking in yeast (Shohdy et al., 2005). In 2012, Shuman and colleagues found that VipA interacts with actin and mildly promotes actin polymerization without the requirement of any other bacterial or host proteins. Additionally, the ability to bind to actin is essential for VipA to localize to actin-rich patches and early endosomes as well as to modulate the endocytic trafficking pathways (Franco, Shohdy et al., 2012).

In summary, at least three *L. pneumophila* type IV effectors have been shown to modulate actin cytoskeleton by distinct mechanisms. However, there is no study which comprehensively investigates the effect of each *L. pneumophila* Dot/Icm effector on host actin cytoskeleton. Considering the importance of the actin cytoskeleton in cellular processes (Pollard & Cooper, 2009) and extensive functional redundancy among *L. pneumophila* effectors**,** I hypothesized that additional Dot/Icm effectors function to target the actin cytoskeleton. In a screening for Dot/Icm substrates capable of modulating the actin cytoskeleton, I identified two effectors- RavK and RavJ, which upon ectopic expression in mammalian cells induce strong actin rearrangement phenotypes. I further investigated the mechanism of action of RavK.

# CHAPTER 2. A *LEGIONELLA* EFFECTOR DISRUPTS HOST CYTOSKELETAL STRUCTURE BY CLEAVING ACTIN


## Abstract

Actin is a core component of the actin cytoskeleton, which plays a crucial role in diverse cellular processes including cell migration, cytokinesis, endocytosis and vesicle trafficking. Therefore, it is not surprising that many pathogens target actin and/or proteins involved in the regulation of actin activity for their benefit. *Legionella pneumophila,* the etiological agent of Legionnaires' disease, uses the Dot/Icm type IVB secretion system to transfer effectors into host cells to subvert host cellular processes for its intracellular replication. At least three Dot/Icm substrates, VipA, Ceg14 and LegK2 have been shown to modulate the host actin cytoskeleton. Here, by screening *L. pneumophila* Dot/Icm substrates that alter the actin cytoskeleton in mammalian cells, we have identified RavK as an additional effector that specifically disrupts actin organization. RavK harbors a canonical metalloprotease motif, which is essential for the RavK-mediated actin cytoskeleton disruption and cell- rounding phenotypes. We further demonstrate that RavK directly cleaves actin, generating a fragment with a diminished capacity to form actin filaments. Our results reveal a new mechanism for which an intravacuolar bacterium disrupts actin cytoskeleton through the cleavage of the actin molecule, rather than interfering with the endogenous actin regulation pathways or by posttranslational modification of the actin molecule, to benefit its intracellular life cycle.


## Introduction

The 42-kDa actin protein assembles into filaments within cells to construct a pervasive and dynamic cytoskeleton, which plays a crucial role in diverse cellular processes including cell migration, cytokinesis, endocytosis and vesicle trafficking (Pollard & Cooper, 2009). Therefore, it is not surprising that many pathogens have evolved effective strategies to target actin and/or proteins involved in the regulation of actin activity. Intracellular bacterial pathogens such as species of *Listeria*, *Shigella*, *Rickettsia* and *Burkholderia* take advantage of distinct host actin polymerization machineries to facilitate their movement within the host cytosol and/or their cell-to-cell spread (Welch & Way, 2013). *Salmonella enterica* Typhimurium modulates the actin cytoskeleton to gain entry into non-phagocytic cells (Galan, 2001). *Chlamydia trachomatis* coopts

the function of actin filaments and intermediate filaments to stabilize its replicative vacuole in epithelial cells (Kumar & Valdivia, 2008). Apart from these, bacterial proteins directly modifying actin monomers have also been identified. The best-studied modification is ADP-ribosylation of actin by the C2 toxin from *Clostridium botulinum*, which modifies Arg-177 of actin, leading to the inhibition of actin polymerization (Aktories, Barmann et al., 1986). In contrast, the *Photorhabdus luminescens* Tc toxin ADP-ribosylates the Thr-148 residue to promote actin polymerization, facilitating the formation of actin aggregates (Lang, Schmidt et al., 2010). Bacterial proteins that cleave actin have also been identified; the metalloprotease ECP32 from *Serratia proteamaculans* cleaves actin, and ectopic expression of this protein enables nonpathogenic *E. coli* to invade eukaryotic cells (Bozhokina, Tsaplina et al., 2011).

Targeting host actin cytoskeleton by *L. pneumophila* virulence factors has emerged as an exciting area of research. At least three *Legionella* Dot/Icm substrates have been shown to modulate distinct cell biological aspects of actin cytoskeleton components. VipA is an actin nucleator, which localizes to actin patches and endosomes during infection and promotes actin polymerization (Franco et al., 2012); Ceg14 co-sediments with filamentous actin and inhibits actin polymerization by an unknown mechanism (Guo, Stephenson et al., 2014a); LegK2 is a kinase that phosphorylates ArpC1b and Arp3, two subunits of the Arp2/3 complex, thus inhibiting actin polymerization on the LCV (Michard et al., 2015). Considering the importance of the actin cytoskeleton in cellular processes and extensive functional redundancy among *Legionella* effectors**,** we hypothesized that more Dot/Icm effectors function to target the actin cytoskeleton. In a screening for Dot/Icm substrates capable of modulating the actin cytoskeleton, we identified RavK as an effector that disrupts the actin cytoskeleton of mammalian cells. We further provide evidence that RavK is a zinc-dependent metalloprotease that specifically cleaves actin and abolishes its polymerization activity. Together with earlier reports on VipA, LegK2 and Ceg14, our results add to a growing body of evidence that *L. pneumophila* utilizes multiple proteins to modulate different aspects of the host actin cytoskeleton in its intracellular life cycle

## Results

### RavK is a *Legionella* effector that disrupts the actin cytoskeleton in mammalian cells

To identify effectors that target the actin cytoskeleton, we screened a GFP fusion library of Dot/Icm substrates (Zhu, Hammad et al., 2013) for their ability to alter the morphology of the

mammalian actin cytoskeleton. Given the essential role of the actin cytoskeleton in cell viability, disruption of its structure most likely is detrimental; we thus began our screening by examining the effects of Dot/Icm substrates known to be toxic to yeast (Guo et al., 2014a, Isberg et al., 2009, Shen, Banga et al., 2009, Tan et al., 2011). From the first eight candidates screened, we found that ectopic expression of effector RavK (Lpg0969) led to the abolishment of the actin cytoskeleton in COS-1 cells (**Fig. 2-1, A)**. Interestingly, overexpression of Lpg0944 caused a detectable rearrangements of actin cytoskeleton with more F-actin accumulating on the plasma membrane (**Fig. 2-1, B)**. In contrast, cells transfected to express the other 6 effectors showed only very minor or undetectable changes in the structure of the actin cytoskeleton compared with those expressing GFP (**Fig. 2-1, C-D; Fig. 2-2**). The strong and clear phenotype associated with RavK prompted us to further investigate its mechanism of action.

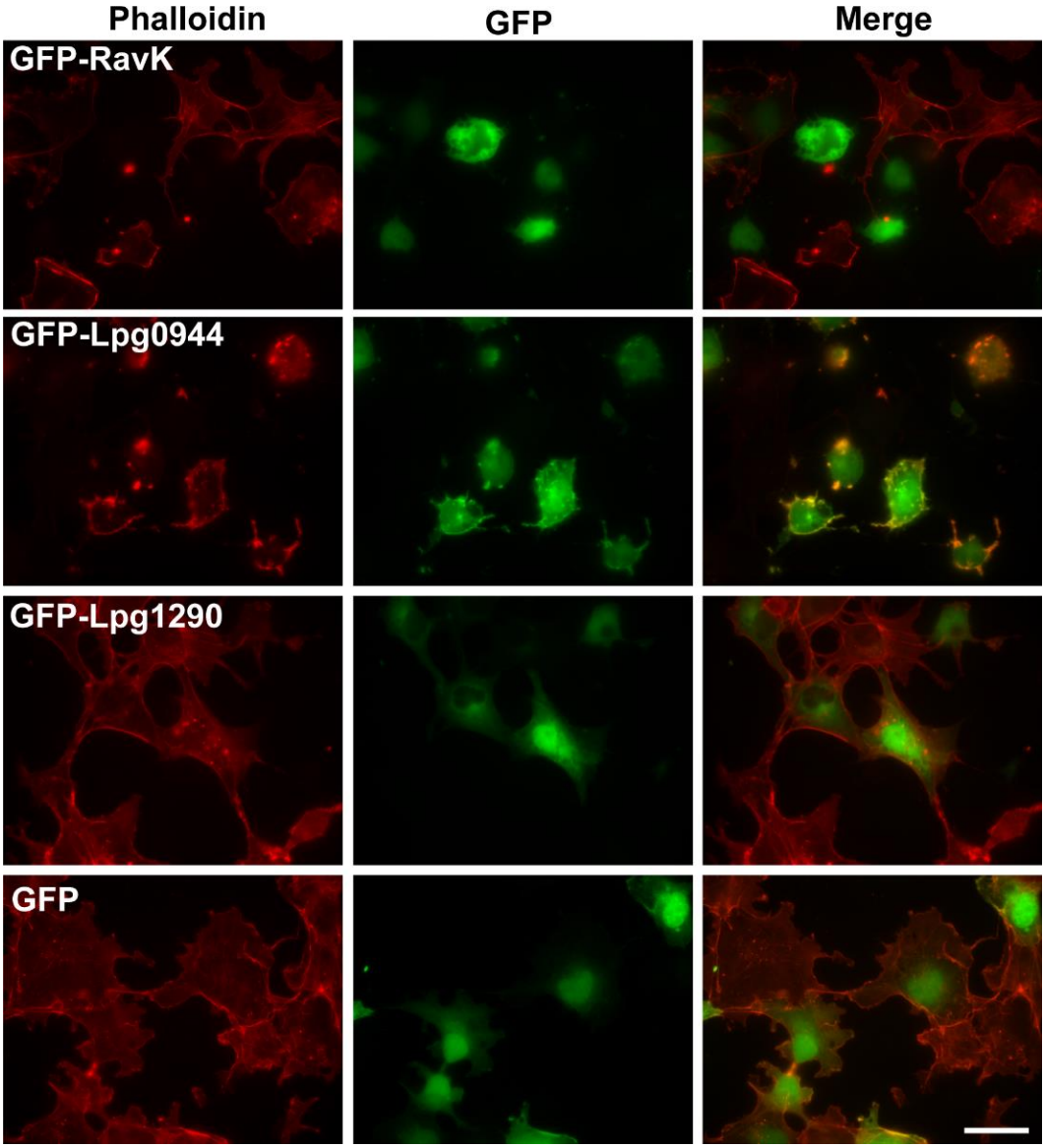


**Fig. 2-1 Identification of *L. pneumophila* Dot/Icm substrates capable of altering the architecture of the actin cytoskeleton of mammalian cells.**
COS-1 cells were transfected to express GFP or GFP fusion of RavK, Lpg0944 and Lpg1290 for 24 h and fixed cells were subjected to staining with Texas-red-conjugated phalloidin. Images shown were from one representative experiment and similar results were seen in three independent experiments. Note that RavK severely reduced the phalloidin signals and that GFP-Lpg0944 caused a rearrangement of the actin cytoskeleton with an increase in cortical actin abundance. In contrast, expression of Lpg1290 did not cause any significant change in the actin cytoskeleton. The cells expressing GFP served as a control. Bar, 20 μm.

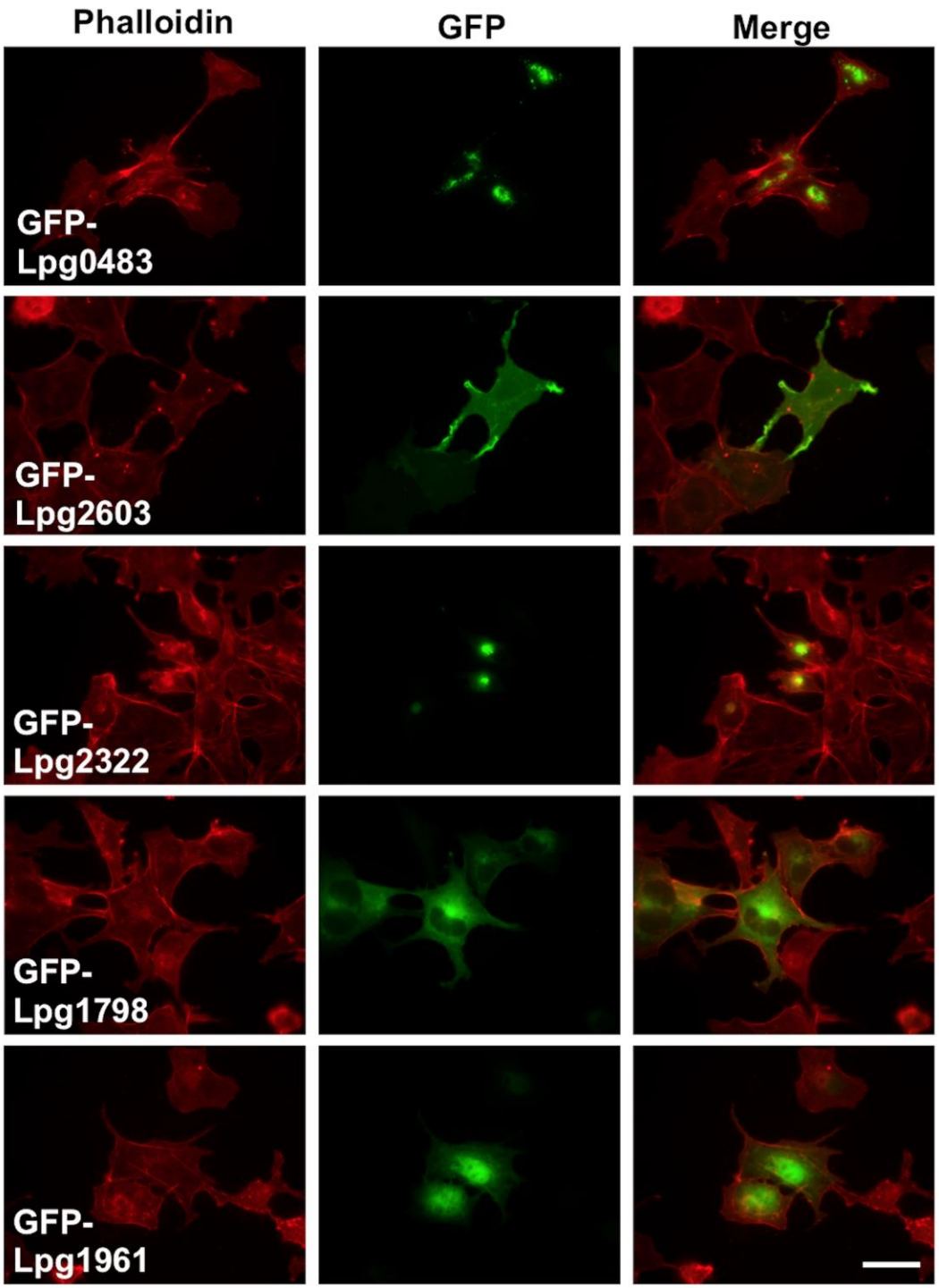


**Fig. 2-2 Identification of *L. pneumophila* effectors that alter the architecture of the actin cytoskeleton of mammalian cells.**
COS-1 cells were transfected by the indicated plasmids for 24 hours and cells were fixed and subjected to staining with Texas-red-conjugated phalloidin. Representative images were shown. Bar, 20 μm.

**RavK is a substrate of the Dot/Icm transporter whose expression is induced at the exponential phase**

RavK was originally identified in a screening for *L. pneumophila* Dot/Icm substrate by its ability to restore the translocation of the transfer-deficient mutant SidCΔC100, and therefore was designated as RavK (*r*egion *a*llowing *v*acuole *c*o-localization K) (Huang et al., 2011). Dot/Icm-dependent translocation of RavK was independently demonstrated using the CCF4/β-lactamase reporter assay (Zhu, Banga et al., 2011a).

Probably due to the need for effectors that effectively thwart the host defense in the initial phase of infection, the expression of many Dot/Icm substrates is induced during the post-exponential phase, when *L. pneumophila* concomitantly enters the transmissive phase and becomes primed for a new round of infection (Isberg et al., 2009). We therefore examined the level of RavK at different time points throughout the growth cycle of *L. pneumophila* in broth. Interestingly, the expression of RavK was highly induced in exponentially growing bacteria (6-18 h) ($OD_{600}$ between 0.4 and 3.0); the protein was barely detectable in the lag (0-6 h) or the post-exponential phase (18-24 h) (**Fig. 2-3**), which indicates that RavK likely plays a role in the replicative phase during *L. pneumophila* infection.

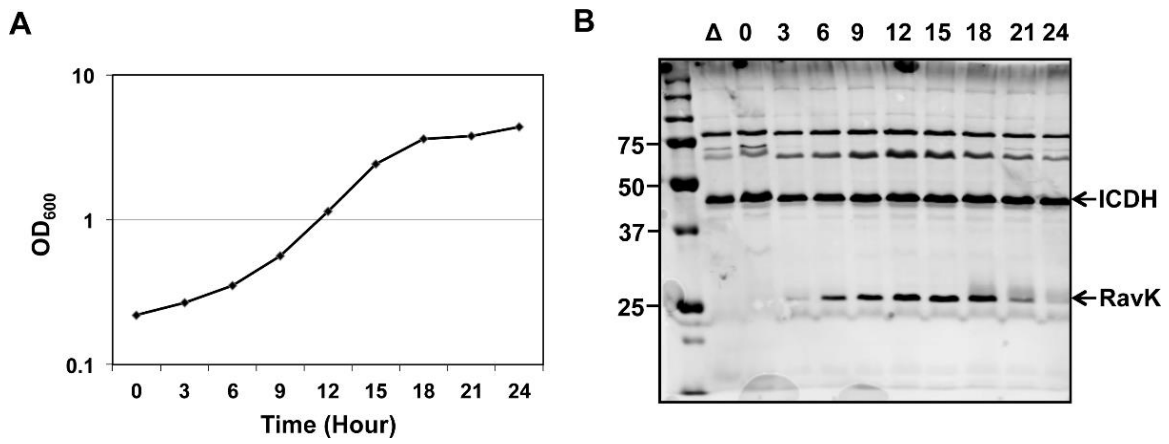


**Fig. 2-3 Expression of RavK is induced in the exponential phase of bacterial growth.**
**A**. The growth of *L. pneumophila* in AYE broth. Cultures grown to stationary phase were diluted 1:20 into fresh medium and the growth of bacteria was monitored by measuring $OD_{600}$ at the indicated time points. **B**. RavK protein level peaked at exponential growth phase. Lysates were prepared from equal amounts of cells withdrawn at the indicated time points and were resolved by SDS/PAGE, and the levels of RavK were examined by immunoblotting with a RavK-specific antibody. The metabolic protein isocitrate dehydrogenase (ICDH) was probed as a loading control.

**An $HE_{XX}H$ motif is essential for the toxicity of RavK and its disruption of the host cytoskeleton**

To understand the mechanism of action of RavK, we first performed sequence analysis of the protein to search for the presence of motifs suggestive of known biochemical activity. We manually scanned the sequence of RavK against the "PROSITE collection of motifs" (Sigrist, de Castro et al., 2013), and found that RavK harbors an $H_{95}E_{XX}H_{99}$ motif present in diverse metalloproteases (Jongeneel, Bouvier et al., 1989) (**Fig. 2-4, A**). To determine the role of this motif in the activity of RavK, we introduced mutations in $H_{95}$, $E_{96}$ and $H_{99}$, respectively. Next, we assessed the effects of these mutations on the activity of RavK by examining their toxicity to yeast; while not affecting the stability of RavK, each of these mutations completely abolished the toxicity to yeast (**Fig. 2-4, B-C**). To examine whether the $H_{95}E_{XX}H_{99}$ motif is required for the disruption of actin cytoskeleton, we expressed GFP-RavK, GFP-$RavK_{H95A}$ or GFP in COS-1 cells and labeled the actin cytoskeleton with Texas-red-conjugated phalloidin. Relative F-actin levels in transfected cells were analyzed by calculating the integrated pixel density of phalloidin fluorescence of outlined individual cell. Our results indicate that the total F-actin levels in GFP-RavK-expressing cells were significantly lower than those in cells expressing GFP or GFP-$RavK_{H95A}$ (**Fig. 2-4, D-E**). We also found that cells expressing GFP-RavK were significantly smaller than that those expressing GFP or GFP-$RavK_{H95A}$ (**Fig. 2-4, F**), indicating that ectopic expression of RavK caused shrinkage in COS-1 cells.

In comparison to the RavK-mediated morphological alterations in COS-1 cells, ectopic expression of GFP-RavK caused a clear cell-rounding phenotype in HEK293T cells. Consistently, the observed phenotype in HEK293T cells also depends on the $H_{95}E_{XX}H_{99}$ motif (**Fig. 2-5**). The different responses to RavK by COS-1 and HEK293T cells may be due to the expression level, variations in the cellular level of the protein targeted by RavK, or a combination of both. Nevertheless, these results suggest that RavK is a metalloprotease that potentially target components of the host cytoskeleton.

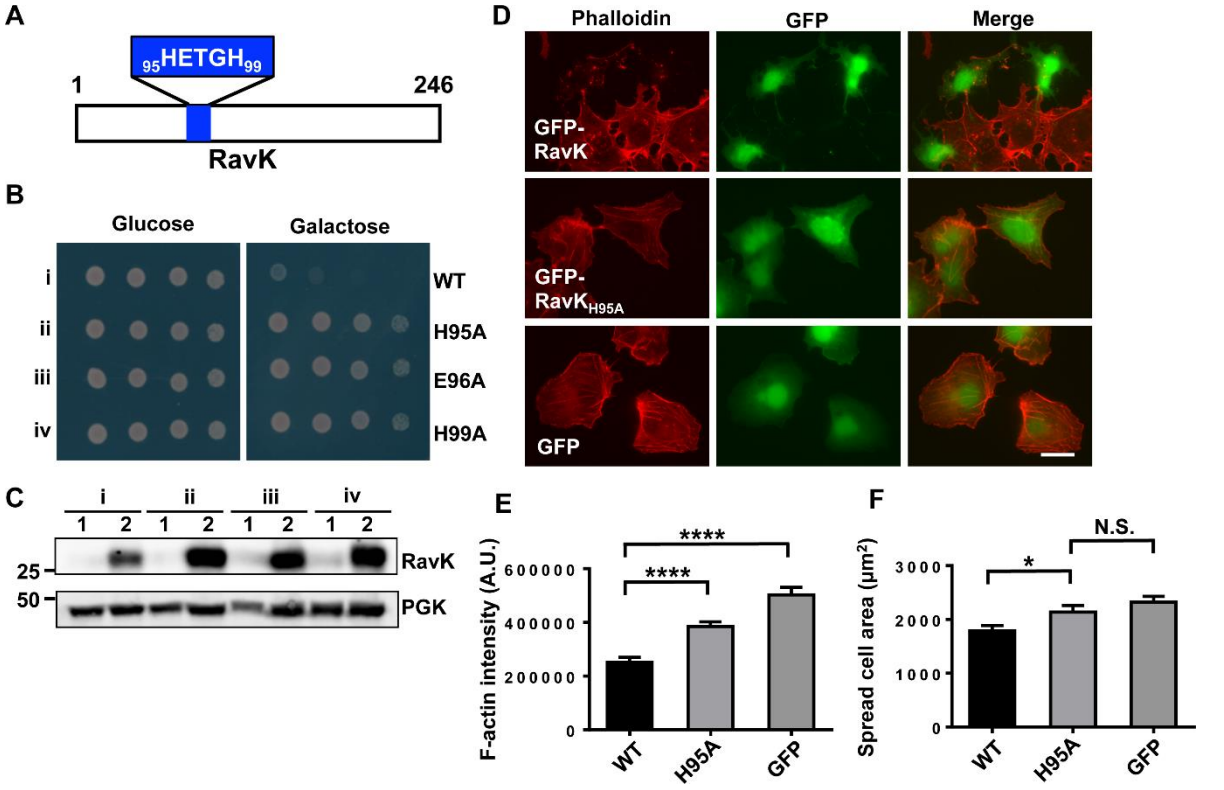


**Fig. 2-4 Expression of RavK causes cytotoxicity in both yeast and mammalian cells and reduces the F-actin content in mammalian cells.**

**A**. A schematic diagram of RavK. The blue box highlighted the position and the sequence of the predicted $HE_{XX}H$ motif. **B**. Expression of RavK induces yeast growth arrest in an $H_{95}E_{XX}H_{99}$-dependent manner. Yeast strains expressing RavK or the indicated mutants under the control of the galactose-inducible promoter were serial-diluted and spotted onto plates containing glucose or galactose, respectively. Plates were incubated at 30℃ for 48 h before image acquisition. **C**. Expression of RavK and the indicated mutants in yeast. Yeast strains grown in glucose medium to saturation were washed with water 5 times and split equally to 2 halves. One half was frozen immediately (sample 1), the other half was induced in galactose medium for 8 h (sample 2). Total proteins of all samples were resolved by SDS/PAGE and probed by immunoblotting with a RavK-specific antibody. The 3-phosphoglycerate kinase (PGK) was used as a loading control. **D**. RavK reduces F-actin content in COS-1 cells. COS-1 cells transfected by the indicated plasmids for 24 h were fixed and subjected to Texas-red-conjugated phalloidin staining. Images from one representative were shown and similar results were obtained in at least three experiments. Bar, 20 μm. **E**. Integrated pixel density of phalloidin staining in cells expressing indicated proteins plotted as average F-actin intensity per cell. N>60 per condition; error bars represent standard error of the mean (SEM); A.U., arbitrary units; ****, $p<0.0001$. **F**. The spread cell area of cells expressing indicated proteins plotted as average area per cell. N>60 per condition; N.S., not significant; *, $p<0.05$.

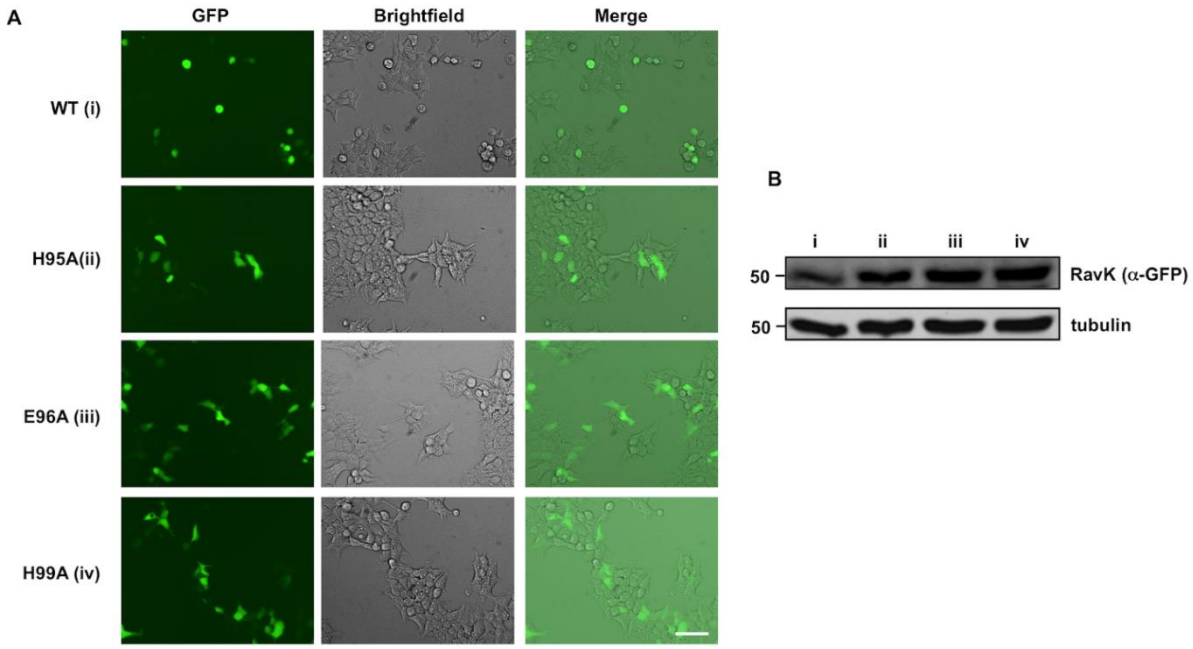


**Fig. 2-5 The $H_{95}EXXH_{99}$ motif is essential for toxicity of RavK toward mammalian cells.**
**A**. HEK293T cells were transfected to express GFP fusion of RavK, $RavK_{H95A,}$ $RavK_{E96A}$ or $RavK_{H99A}$ for 16 h and the images were acquired by a fluorescence microscope. Bar, 50 μm. **B.** Expression of GFP fusions in samples from A. Total cell lysates resolved by SDS-PAGE were probed with antibodies specific for GFP (for the GFP fusion to RavK and its derivatives) and for tubulin as a loading control.

**Expression of RavK reduces the total actin level in mammalian cells**

Actin exists in cells as both free monomer, called G-actin (globular actin), and as polymeric microfilaments, called F-actin (filamentous actin) (Dominguez & Holmes, 2011). The RavK-induced reduction of the phalloidin-stainable F-actin in COS-1 cells can be accounted for by at least two possibilities. First, RavK directly reduces the total pool of actin within the cells by mechanisms such as proteolytic cleavage. Second, RavK somehow tilts the balance toward G-actin and reduces the pool of F-actin. To distinguish between these two possibilities, we compared the total actin level between cells expressing RavK and the $RavK_{H95A}$ mutant and found that cells expressing wild-type RavK contained much lower levels of total actin than that of cells expressing $RavK_{H95A}$ or GFP (**Fig. 2-6, A-B**), indicating that RavK reduces the abundance of total actin in COS-1 cells. Similarly, RavK expression also reduced total actin level in HEK293T cells (**Fig. 2-7, A-B**).

**RavK is a protease that cleaves actin**

The reduction of cellular actin levels by RavK can be caused by directly degrading the protein or by initiating a signaling cascade that leads to lower cellular actin levels. A direct approach to distinguish between these two models is by incubating recombinant RavK with total lysates of mammalian cells and examining the levels of actin. To obtain active RavK protein for such biochemical assays, we made numerous attempts to express epitope-tagged RavK for affinity purification from *E. coli*, none of the used tags such as $His_6$, $His_6$-Sumo, and GST allowed us to obtain soluble full-length RavK (**Fig. 2-8, A**). We therefore initiated a screening to identify truncated alleles of RavK that would potentially be soluble and functional for biochemical studies. A series of RavK deletion mutants were constructed by removing residues from its C-terminal end (the $H_{95}EXXH_{99}$ motif localizes toward its N-terminal portion). Whereas deletion of 50 residues from the C-terminal end led to a mutant that retained the toxicity to yeast, a mutant lacking 100 amino acids from the same end abolished its toxicity (**Fig. 2-8, B-C**). Consistent with its toxicity to yeast, RavKΔC50 still caused cell rounding in HEK293T cells (**Fig. 2-8, D-E**). Notably, the ΔC50 deletion greatly increased the solubility of RavK, which allowed us to obtain sufficient recombinant protein for biochemical experiments (**Fig. 2-8, A**).

To determine the activity of the recombinant RavKΔC50, we incubated lysates of COS-1 cells with $His_6$-RavKΔC50 or $His_6$-$RavK\Delta C50_{H95A}$ at 22ºC for 1 h. Wild type RavKΔC50 but not

the H95A mutant caused a reduction of full-length actin and produced an actin fragment clearly smaller than the original protein in the cell lysates. Furthermore, the reduction of actin can be inhibited by the metal ion chelator EDTA (**Fig. 2-6, C**). Similar results were observed with lysates of HEK293T cells (**Fig. 2-7, C**). Thus, RavK is a metalloprotease, which is able to cleave actin in lysates of mammalian cells in an $H_{95}ExxH_{99}$ motif-dependent manner.

We next tested whether any host factor is required for the cleavage of actin by RavK by mixing human non-muscle actin (85% β-actin and 15% γ-actin) with $His_6$-RavKΔC50 or $His_6$-RavKΔC50$_{H95A}$ for various time durations. Incubation with $His_6$-RavKΔC50 but not with the H95A mutant produced a smaller actin fragment (**Fig. 2-6, D**) and the size difference between these two fragments is similar to that observed in experiments using total cell lysates. Consistent with earlier observations, the activity of RavK is sensitive to EDTA. Thus, RavK is a metalloprotease that cleaves actin without the requirement of any other host proteins.

Among the three major groups of actin (α, β, γ) identified in vertebrates, the α-actin is the major constituent of the contractile apparatus in muscle cells, whereas the β and γ actin coexist in most of non-muscle cells as a component of cytoskeleton (Herman, 1993). We thus tested whether RavK has a preference toward specific actin isoforms. Since the protein sequence of commercially available rabbit skeletal muscle actin is identical to that of human skeletal muscle actin, we used rabbit muscle actin in this assay for comparison to human non-muscle actin. The same amount of rabbit muscle actin and human non-muscle actin was treated with equal amount of $His_6$-RavKΔC50. As early as 2 min post treatment, significantly more cleaved product was detected in reactions with non-muscle actin than those with muscle actin. When the reaction was allowed to proceed for 128 min, more than 80% of non-muscle actin was cleaved, whereas only approximately 25% of muscle actin that was cleaved in this experimental duration (**Fig. 2-6, E-F)**. Thus, RavK cleaves the non-muscle actin more efficiently than the muscle actin.

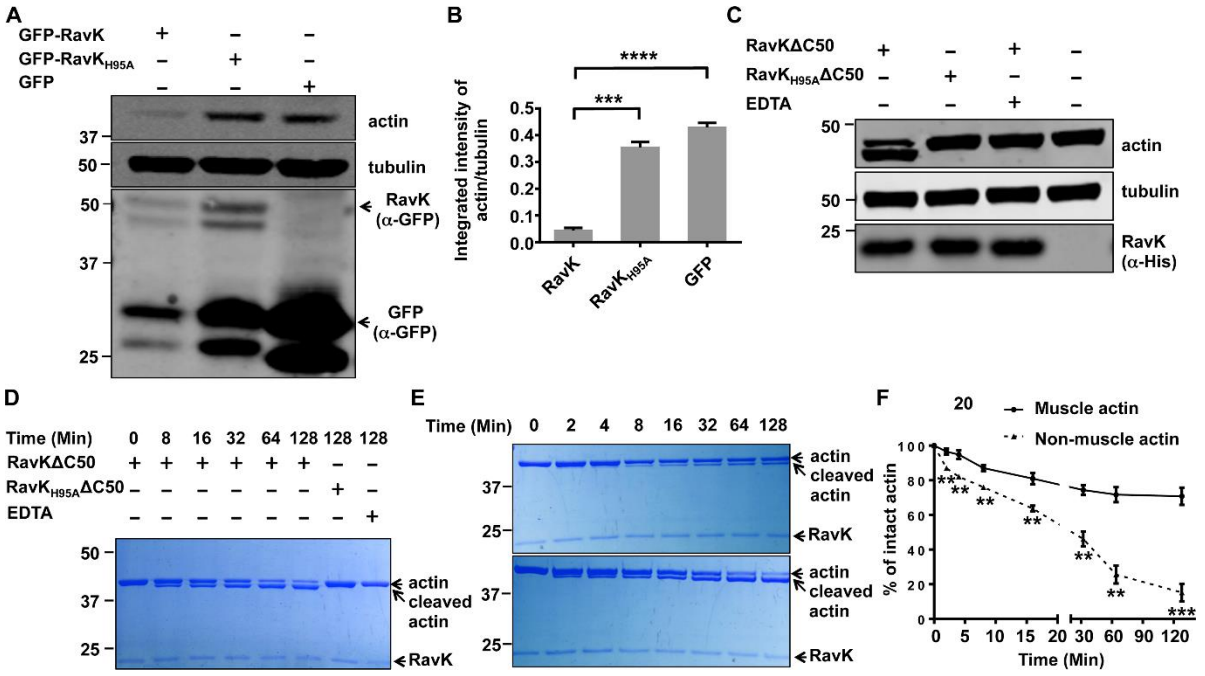


**Fig. 2-6 The cleavage of actin by RavK.**

**A**. Expression of RavK reduced the level of actin in COS-1 cells. Indicated proteins were expressed in COS-1 cells for 24 hours and cleared cell lysates were subjected to SDS/PAGE and immunoblotting with GFP-specific and actin-specific antibodies, respectively. α-tubulin was probed as a loading control. **B**. The intensity of the bands corresponding to actin and tubulin was measured with ImageJ and the intensity ratio between actin and tubulin revealed the relative actin level in cells of the relevant samples. All results are from three independent experiments. Error bars represent standard error of the mean (SEM). ***, $p$<0.001, ****, $p$<0.0001. **C**. Recombinant RavKΔC50 cleaved actin in lysates of COS-1 cells. Indicated proteins were added to COS-1 cell lysates and the reactions were allowed to proceed for 1 h at 22℃, EDTA was added to the indicated samples. Samples were separated by SDS/PAGE and detected by immunoblotting with an actin-specific antibody. α-tubulin was probed as a loading control. **D**. Recombinant RavKΔC50 cleaved actin *in vitro* in an HE$_{XX}$H motif-dependent manner. 10-μg human non-muscle actin was incubated with 1-μg RavKΔC50 or RavK$_{H95A}$ΔC50 for the indicated time and the mixtures separated by SDS/PAGE were stained with Coomassie brilliant blue. EDTA was added into the samples at the beginning when indicated. **E**. The cleavage of human non-muscle actin and rabbit muscle actin by RavKΔC50. The *in vitro* cleavage was performed similarly as described in C. Upper panel: Muscle actin; Lower panel: Non-muscle actin. **F.** RavKΔC50 cleaves human non-muscle actin more efficiently than rabbit muscle actin. The percentage of intact actin/total actin was calculated with ImageJ. All results were from three independent experiments. *, $p$<0.05, ***, $p$<0.001.

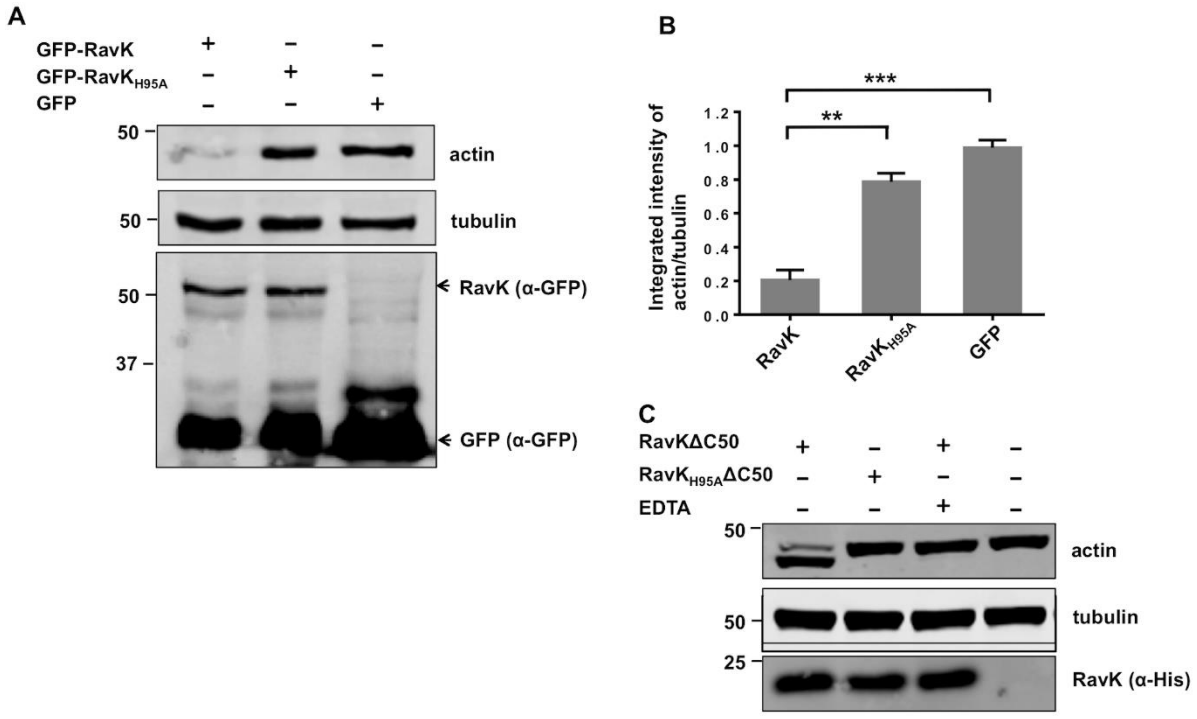


**Fig. 2-7 RavK reduces the actin level in HEK293T cells.**
**A.** Expression of RavK reduces the level of actin in HEK293T cells. Cell transfection and immunoblotting were performed similarly as **Fig. 2-6, A**. **B.** Quantification of the band intensity ratio of actin versus tubulin as described in **Fig. 2-6, B**. All results are from three independent experiments. Error bars represent SEM. ****,** $p$<0.01, *****,** $p$<0.001. **C.** Recombinant RavKΔC50 cleaves actin in COS-1 cell lysates. Cleavage and immunoblotting were performed as described for **Fig. 2-6, C**.

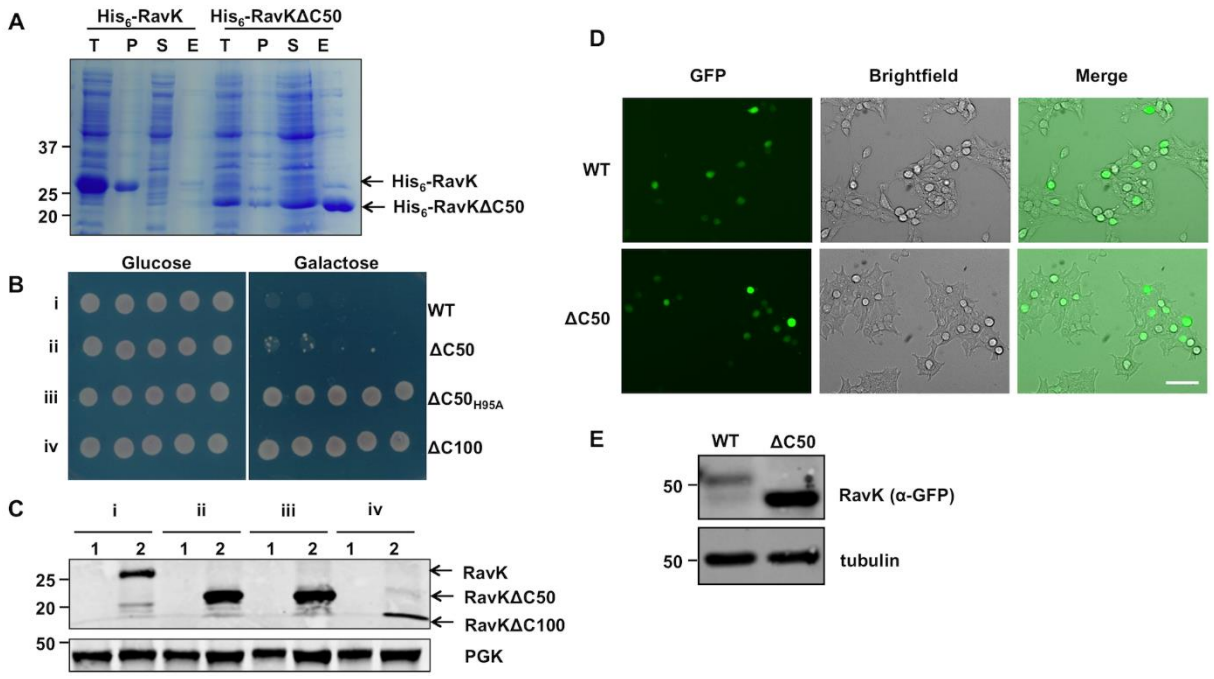


**Fig. 2-8 Deletion of 50 residues from the C-terminal end of RavK allowed the purification of active protein.**

A. Expression of RavK and RavKΔC50 in *E. coli*. Note that RavKΔC50 is more soluble than RavK. T, Total lysate; P, Pellet; S, Supernatant; E, Elution. **B.** RavKΔC50 but not RavKΔC100 inhibits yeast growth. Yeast toxicity assay was performed as described in **Fig. 2-4, B**. **C.** Expression of RavK and indicated mutants in yeast. Total proteins of the indicated yeast strains induced with galactose as described in **Fig. 2-4, C** were probed by immunoblotting for RavK and the PGK kinase was probed as a loading control. **D-E.** The toxicity of RavKΔC50 to mammalian cells. GFP fusion of full-length or RavKΔC50 was expressed in 293T cells and the images were acquired 16 h after transfection (D), the expression of the fusions were probed with an antibody specific for GFP (E) and tubulin was probed as a loading control.

As RavK harbors an $H_{95}E_{XX}H_{99}$ motif that is common for zinc binding, we further tested whether zinc is required for the activity of RavK. Seven different metal ions including zinc were tested for their ability to restore the activity of metal ion-free RavK. Indeed, $Zn^{2+}$ was able to restore the activity of RavK (**Fig. 2-9**). Notably, whereas such divalent ions as $Co^{2+}$, $Ni^{2+}$, $Cu^{2+}$, $Ca^{2+}$ or $Mg^{2+}$ cannot detectably restore the activity of RavK, $Mn^{2+}$ was able to restore the activity of RavK at levels comparable to those of $Zn^{2+}$, probably due to their similarity in chemical properties (Bock, Katz et al., 1999).

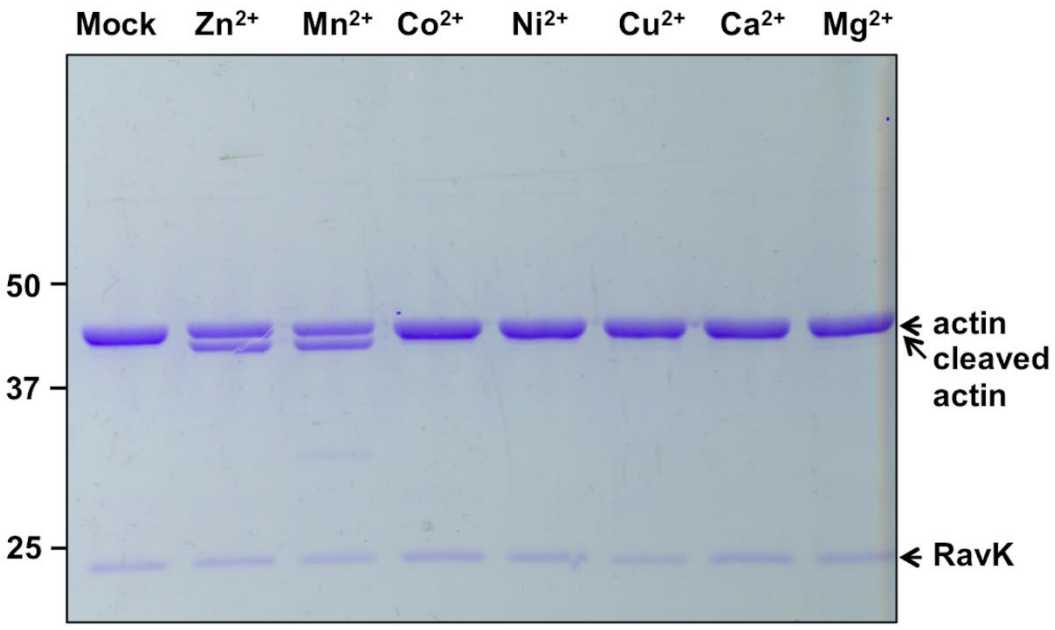


**Fig. 2-9 The effects of several divalent metal ions on the activity of metal-free RavK.**
The indicated metal ions were individually added to reactions containing actin and $His_6$-RavKΔC50 treated with EDTA. 2 h after incubation, the enzymatic activity was assessed by detecting the production of cleaved actin after SDS-PAGE and Coomassie brilliant blue staining. Similar results were obtained in three independent experiments.

**RavK-dependent cleavage of actin during *L. pneumophila* infection**

To investigate whether the RavK-mediated cleavage of actin occurs during bacterial infection, we infected mammalian cells expressing 4xFlag-tagged actin with wild-type *L. pneumophila* or its derivatives. Cleaved actin was only detected in samples infected with the *ΔravK* strain expressing RavK from a multi-copy plasmid but not in samples infected by the Δ*ravK* strain or *ΔravK* overexpressing $RavK_{H95A}$, indicating that actin is cleaved during *L. pneumophila* infection in a RavK-dependent and more specifically metalloprotease motif-dependent manner (**Fig. 2-10, A**). The cleaved form of actin was not observed in samples infected by wild-type *L. pneumophila*, which may be attributed to less translocated RavK in host cytosol compared to samples infected by *ΔravK* overexpressing RavK. Considering the expression level of RavK is much higher in *ΔravK* overexpressing RavK than in wild-type *L. pneumophila* (**Fig. 2-10, B**), it is almost certain that more RavK was translocated to host cells by the overexpressing strain, which caused detectable cleavage of Flag-actin. Yet, in both cases the amount of translocated RavK was below the detection capacity of immunoblotting with our RavK-specific antibody (**Fig, 2-10, C**). Despite multiple attempts using different infection conditions such as variations in multiplicity of infection (MOI), infection time and host cells, we were unable to detect the cleavage of endogenous actin even in infections using the strain overexpressing RavK (**Fig. 2-10, D**). The inability to detect the reduction of actin or the cleaved product may attribute to low stability of the cleaved product in cells, the quality of the antibodies used for detection or the potential compensatory effects from the hosts, or a combination of these factors.

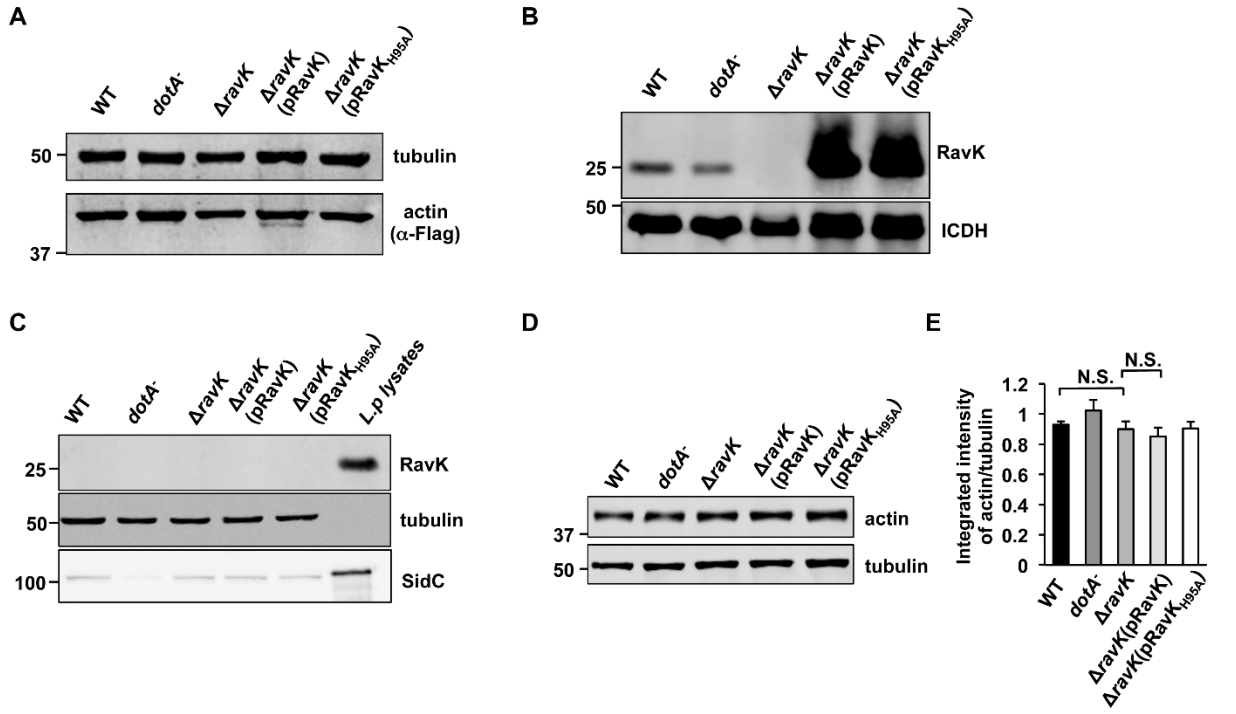


**Fig. 2-10 RavK-mediated cleavage of actin occurs during *L. pneumophila* infection.**
**A**. Actin is cleaved by translocated RavK during bacterial infection. Cells expressing Flag-tagged actin were infected with relevant *L. pneumophila* strains for 2 h and cleared cell lysates was probed by immunoblotting with a Flag specific antibody. Tubulin was probed as a loading control. Similar results were obtained from more than three independent experiments and a representative blot was shown. **B**. The bacteria used for infections were probed for RavK expression, the lysates of WT and *dotA*$^-$ strains were from exponential phase bacteria and the others were from post-exponential phase bacteria; the metabolic enzyme isocitrate dehydrogenase (ICDH) was probed as a loading control. **C**. RavK cannot be detected in saponin-soluble fractions of infected cells with RavK-specific antibody. SidC, a known Dot/Icm substrate was probed as a positive control for translocation and tubulin was probed as a loading control. **D**. Cleavage of endogenous actin. Lysates of cells similarly infected as described in C were probed for actin with tubulin as a loading control (left panel). **E**. The ratio of intensity between the bands representing actin and tubulin was quantified from three independent experiments (right panel). Note that a reduction in actin was not observed even in infections using the RavK overexpressing strain. N.S., not significant.

**Cleavage of actin by RavK occurs at a site between T351 and F352**

To determine the cleavage site of actin by RavK, we incubated non-muscle actin with $His_6$-RavKΔC50 at 22°C for 1 h. Samples resolved by SDS-PAGE were detected by Coomassie brilliant blue staining. Protein bands corresponding to both the uncleaved, full-length and the cleaved products were excised, digested with trypsin and sequenced by mass spectrometry (**Fig. 2-11, A**). Analysis of the detected tryptic fragments revealed that the semi-tryptic peptide -$Y_{337}$SVWIGGSILASLST$_{351}$- was present in the cleaved protein but not in the full length protein, suggesting that the cleavage site lies between Thr351 and Phe352 (**Fig. 2-12, A**). Consistent with this notion, the abundance of the N-terminal peptide -$D_2$DDIAALVVDNGSGMCK$_{18}$- was similar between these two proteins, whereas the abundance of the C-terminal peptide -$Q_{360}$EYDESGPSIVHR$_{372}$- was significantly higher in the full-length protein than in the cleaved product (**Fig. 2-12, A**), further suggesting that the cleavage site identified by this method is reliable. We confirmed the identified cleavage site by mutating Phe352 into an Ala in β-actin. A Flag-tagged β-actin$_{F352A}$ gene was expressed in HEK293T cells by transfection. Immunoprecipitated Flag-β-actin$_{F352A}$ eluted with the Flag peptide was incubated with $His_6$-RavKΔC50 and the cleavage product was detected by immunoblotting with the Flag-specific antibody. RavK treatment of similarly purified wild type Flag-β-actin yielded two protein bands with a molecular weight difference resemblying that observed in experiments with purified actin (**Fig. 2-12, B**). In contrast, only one single protein corresponding to the size of uncleaved actin was detected in samples expressing the actin$_{F352A}$ mutant (**Fig. 2-12, B**), establishing that Phe352 is important for RavK-mediated cleavage. Residues around the cleavage site often provide the structural context important for recognition by proteases (Chisholm, Dahlbeck et al., 2005); we therefore constructed a series of mutants with substitution mutations in sites adjacent to Phe352 and examined their sensitivity to RavK. Our results indicate that Leu349, Ser350, Thr351 are indispensible for RavK-mediated cleavage, whereas Gln353 and Gln354 are not essential (**Fig. 2-12, C**).

With the exception of Ser350, which is replaced by a Thr residue in yeast actin, all the other residues tested in our mutational analysis are conserved among all human actin isoforms and yeast actin (Act1) (**Fig. 2-11, B**). Thus, it is likely that the yeast toxicity of RavK is due to its cleavage of yeast actin. We tested this hypothesis by incubating Flag-Act1 with RavKΔC50. Incubation of wild-type RavK but not the RavK$_{H95A}$ resulted in the production of a smaller Act1 fragment, and the fragment was absent in the reaction receiving EDTA (**Fig. 2-12, D**), indicating

that RavK cleaves Act1 in a metalloprotease activity-dependent manner. Thus, the protease activity against actin attributes to the cytotoxicity of RavK in yeast.

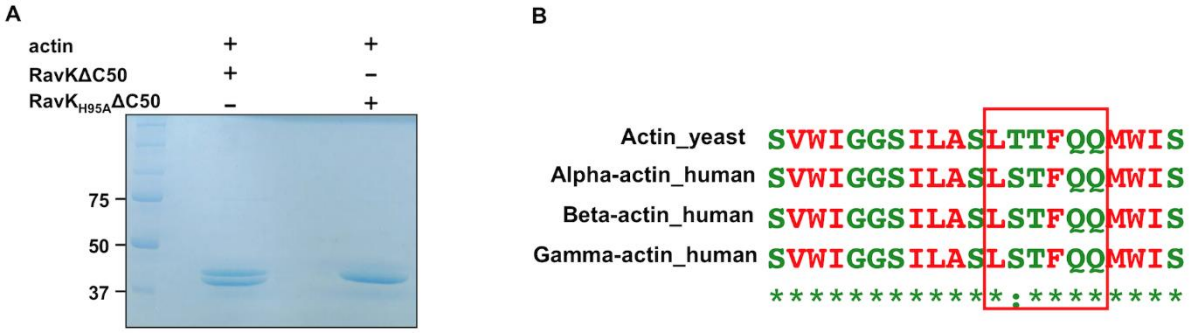


**Fig. 2-11 Preparation of samples for mass spectrometry analysis and the sequence alignment of the RavK recognition site from different forms of actin.**

**A.** Non-muscle actin was incubated with RavK for 1 h, and the protein mixtures were resolved by SDS-PAGE, followed by Coomassie brilliant blue staining. Both upper and lower bands were excised and analyzed by mass spectrometry. **B.** Sequence alignment of yeast actin and the three human actin isoforms. Red box highlighted the six residues examined in **Fig. 2-12, C**.

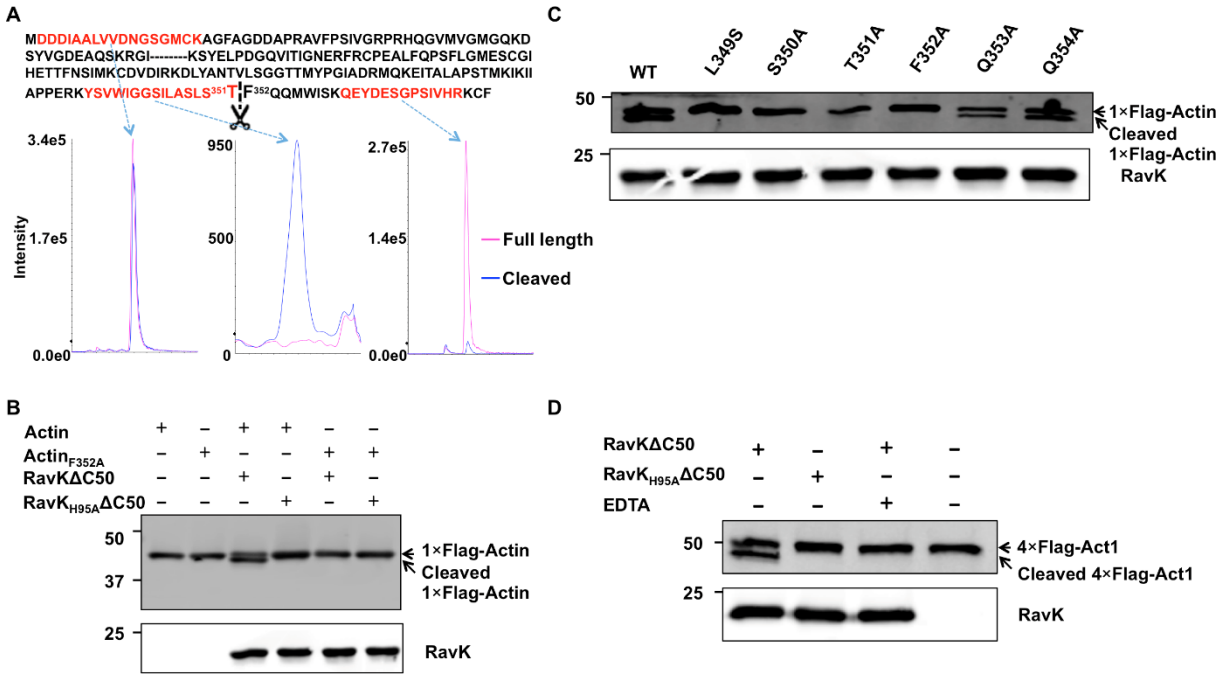


**Fig. 2-12 RavK cleaves β-actin by recognizing a site between T351 and F352.**
**A**. RavK cleaved β-actin at a site between T351 and F352. A portion of actin amino acid sequence containing the relevant peptides was shown. A comparison of the abundance of the semi-tryptic end peptide -YSVWIGGSILASLST- in two bands suggested that the cleavage site lies between T351 and F352. The abundance of two fragments located in the N-terminal and the C-terminal portion of actin, respectively, was compared to validate the results. **B**. The β-actin F352A mutant was resistant to RavK cleavage. HEK293T cells were transfected to express Flag tagged β-actin WT or its F352A mutant. 24 h after transfection, cell lysates were subjected to immunoprecipitation using M2 beads for 3 h. Proteins eluted with 3×Flag peptides were treated by either RavKΔC50 or $RavK_{H95A}$ΔC50 for 2 h and the samples were separated by SDS-PAGE and detected by immunoblotting with Flag-specific antibody. **C**. The Q353A and Q354A mutants of β-actin were still sensitive to RavK. Residues at the indicated positions were mutated and the mutant proteins were individually expressed in HEK293T cells, Flag-tagged proteins obtained as described in (B) were treated with RavKΔ50WT and were subjected to immunoblotting. **D**. The cleavage of yeast actin by RavK. Flag-tagged Act1 expressed in yeast obtained from cell lysates by immunoprecipitation was subjected to RavK cleavage. Samples were separated by SDS-PAGE and detected by immunoblotting with Flag-specific antibody and $His_6$-specific antibody, respectively.

**The actin$_{F352A}$ mutant suppresses the RavK-induced cell rounding**

Actin is one of the most abundant proteins in eukaryotic cells, it is possible that the cleavage by RavK we observed is due to non-specific activity. To test whether actin is a *bona fide* target of RavK, we set out to examine whether overexpressing a cleavage-resistant actin variant in HEK293T cells could rescue the cell rouding phenotype mediated by RavK. Overexpression of the actin$_{F352A}$ mutant did not cause any disernable effects in mammalian cells, suggesting that this mutation did not overtly affect the function of actin. If actin is the true substrate of RavK, cells overexpressing actin$_{F352A}$ should become resistant to damage caused by the protease. Overexpression of wild-type actin did not reduce the percentage of rounded cells induced by RavK, which was similar to samples receiving only the construct for RavK (**Fig. 2-13**). In contrast, overexpression of actin$_{F352A}$ in HEK293T cells almost completely abrogated the cell rounding phenotype, although these cells expressed RavK at levels similar to other samples (**Fig. 2-13)**. The ability of actin$_{F352A}$ to effectively suppress the RavK-induced phenotypes further establishes that actin is a *bona fide* cellular target of RavK.

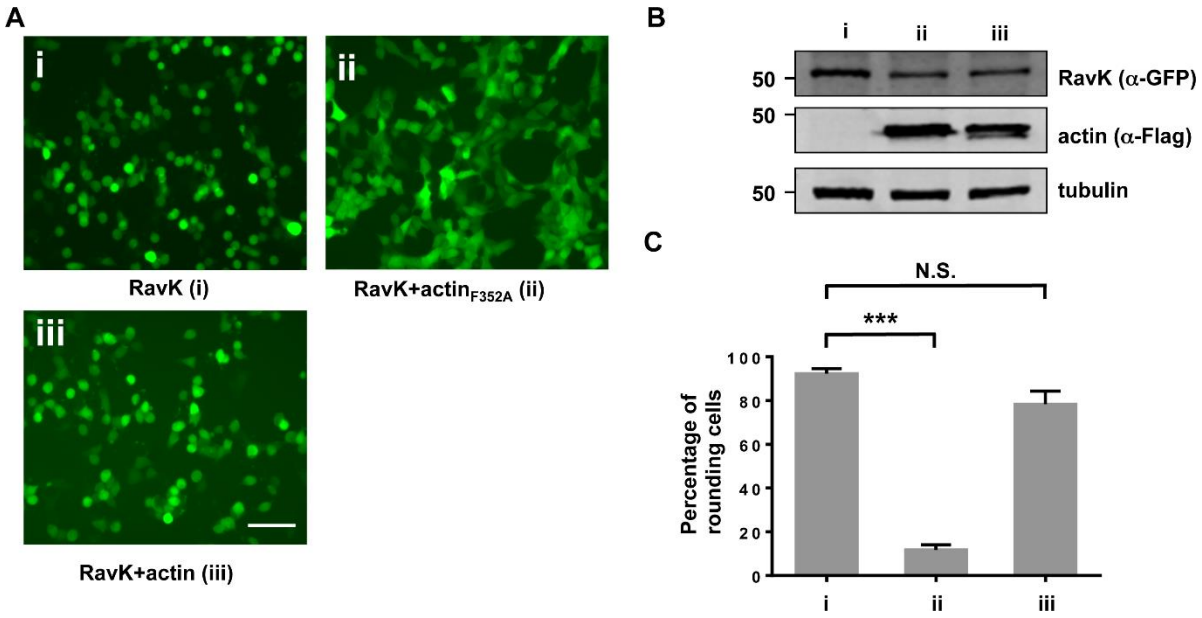


**Fig. 2-13 Actin$_{F352A}$ suppresses the cell rounding phenotype caused by RavK**
**A**. Actin$_{F352A}$ but not wild-type actin suppressed the cell rounding phenotype caused by RavK. HEK293T cells were transfected with (i) pE*gfp-ravK* alone, (ii) pE*gfp-ravK* together with pCMV-Flag-*actin* or (iii) pE*gfp-ravK* together with pCMV-Flag-*actin$_{F352A}$* for 24 h, and were observed under a fluorescence microscope. Bar, 50 μm. **B**. Expression of GFP-RavK, Flag-actin or Flag-actin$_{F352A}$. Cells were transfected by indicated plasmids for 24 h, and the cleared lysates from transfected samples were resolved by SDS/PAGE, and subjected to immunoblotting with antibodies specific to GFP and the Flag tag, respectively. α-tubulin was used as a loading control. **C**. Quantification of the percentage of green cells exhibiting the cell rounding phenotype. Experiments were performed in triplicate and at least 200 cells were examined in each sample. Error bars indicate standard error of the mean (SEM); N.S., not significant; ****, $p$<0.0001. Similar results were obtained in three independent experiments.

**Actin cleaved by RavK is defective in polymerization**

Actin exists as both G-actin and F-actin in the cell and the transition between these two forms in response to cellular needs is precisely regulated (Dominguez & Holmes, 2011). Given the importance of actin polymerization in its function, we tested whether the RavK-cleaved actin retains the ability to form actin filaments. The formation of filaments by G-actin can occur spontaneously under certain conditions, which can be measured by sedimentation after high-speed centrifugation (Namba, Ito et al., 1992). We therefore determined the polymerization activity of actin after RavK-mediated cleavage. As complete cleavage of non-muscle actin by RavK cannot be achieved even after extended incubation, a mixture consisting of cleaved and uncleaved actin was used in this and following assays. Non-muscle actin that had been incubated with RavKΔC50 or $RavK_{H95A}$ΔC50 at 22ºC for 2 h was induced to polymerize for 60 min. The formation of actin filaments was determined by its presence in pellets after ultracentrifugation. Similar to mock-treated actin, in reactions containing actin that had been incubated with $RavK_{H95A}$ΔC50, the majority of actin was in the pellets, indicative of robust polymerization (**Fig. 2-14, A-B**). In contrast, in reactions containing RavKΔC50, only approximately 40% of the actin was present in the pellet, indicating the cleaved product is defective in polymerization.

To further validate our findings based on the high-speed centrifugation assay, we examined the ability of $actin_{1-352}$ to form actin filaments by a pyrene-labeled actin nucleation assay. Two-hour treatment with $RavK_{H95A}$ΔC50 only slightly decreased the polymerization property of non-muscle actin compared with the control samples receiving no additional protein. On the other hand, incubation with RavKΔC50 for the same time duration drastically reduced the ability of actin to form polymers for non-muscle actin **(Fig. 2-14, C-D)**, further confirming RavK-cleaved actin is defective in forming actin filaments.

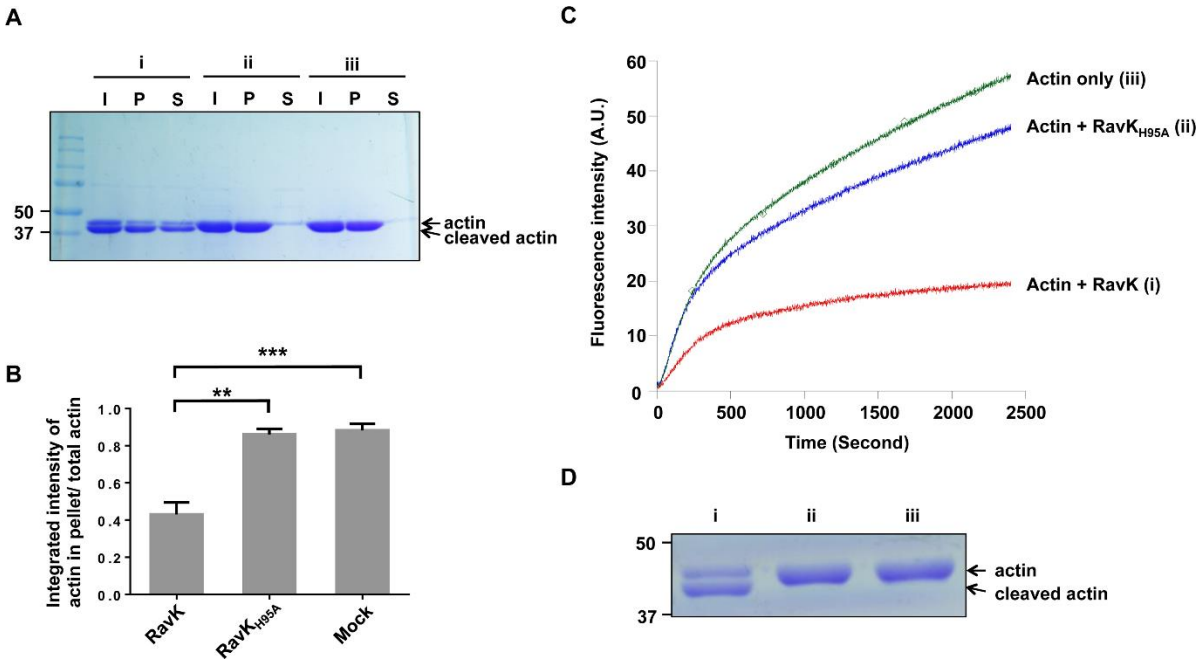


**Fig. 2-14 Cleavage by RavK inhibits actin polymerization.**

**A**. Cleavage by RavK inhibited actin polymerization in actin sedimentation assay. 30-µg non-muscle actin (Cytoskeleton, 99% purity) was incubated with 5-µg wild-type RavKΔC50 or the catalytically dead mutant RavK$_{H95A}$ΔC50 at 23ºC for 2 h. The mixtures were precleared by centrifugation at 100,000*g* for 30 min and further used in actin sedimentation assays. Actin polymerization was allowed to proceed for 60 min, followed by ultracentrifugation at 100,000*g* for 40 min. The resulting supernatants and pellets were analyzed by SDS-PAGE followed by Coomassie brilliant blue staining. Groups: i, actin treated with RavKΔC50; ii, actin treated with RavK$_{H95A}$ΔC50; iii, actin without treatment. Lanes: I, input; P, pellet; S, supernatant. **B**. Quantification of the percentage of polymerized actin versus total actin. The band intensity was quantified with ImageJ. All results are obtained from three independent experiments. Error bars represent standard error of the mean (SEM). **, $p<0.01$. **C**. Cleavage by RavK inhibited actin polymerization in a kinetic assembly assay. Non-muscle actin treated by RavKΔC50, RavK$_{H95A}$ΔC50 or a control reaction with RavK was precleared by centrifugation at 100,000*g* for 30 min. 2.7-µM differently-treated actin and 0.3 µM pyrene-labeled actin were mixed and the fluorescence intensity of pyrene (arbitrary units, a.u.) was plotted versus time after the addition of a polymerization buffer to initiate the polymerization. **D**. Actin used in pyrene-labeled actin polymerization assay. Actin samples receiving indicated treatment were resolved by SDS-PAGE and detected by Coomassie brilliant blue staining.

**RavK is not required for proficient intracellular growth of *L. pneumophila* in macrophages and a protozoan host**

RavK is present in 23 out of 41 sequenced *Legionella* species, and is one of the 74 effectors which are shared by more than 20 different *Legionella* species (Burstein, Amaro et al., 2016). Such a high prevalence suggests an important role of this protein in the interactions of the bacteria with their hosts. To study the role of RavK during *L. pneumophila* infection, we constructed an in-frame deletion mutant of this gene and investigated the intracellular replication of this mutant in primary mouse macrophages and the protozoan host *Dictyostelium discoideum*. Similar to many Dot/Icm substrates, the results show that the absence of RavK does not affect the uptake by host cells or the intracellular replication capacity of *L. pneumophila* in mouse macrophages or *D. discoideum* (**Fig. 2-15, A-B**). It has been reported that two other *Legionella* effectors Ceg14 and VipA also target host actin cytoskeleton. Ceg14 co-sediments with filamentous actin and inhibits actin polymerization (Guo et al., 2014a), whereas VipA is an actin nucleator, promoting actin polymerization (Franco et al., 2012). Since both Ceg14 and RavK negatively affect the actin polymerization, we investigated whether the absence of both of them would cause any intracellular growth defects. The intracellular growth of *ceg14*/*ravK* double knockout strain was determined and the results showed that it still grows as proficiently as the wild-type strain in either mouse macrophages or *D. discoideum* (**Fig. 2-15, A-B**). Recently, the *Legionella* effector LegK2 was shown to inhibit actin polymerization by phosphorylating the Arp2/3 complex (Michard et al., 2015). We therefore made a *ceg14*/*ravK/legk2* triple knockout mutant to examine the potential functional redundancy of these three proteins. The *ceg14*/*ravK/legK2* triple mutant manifests ~10 fold growth defect compared to wild-type strain in *D. discoideum*. However, this defect is comparable to that of the *legK2* mutant (**Fig. 2-15, C**), indicating the absence of RavK and Ceg14 does not confer any further growth defects to the *legK2* mutant. Consistent with this observation, the intracellular growth defect of the triple mutant can be complemented by *legK2* but not *ravK* or *ceg14* (**Fig. 2-15, D**).

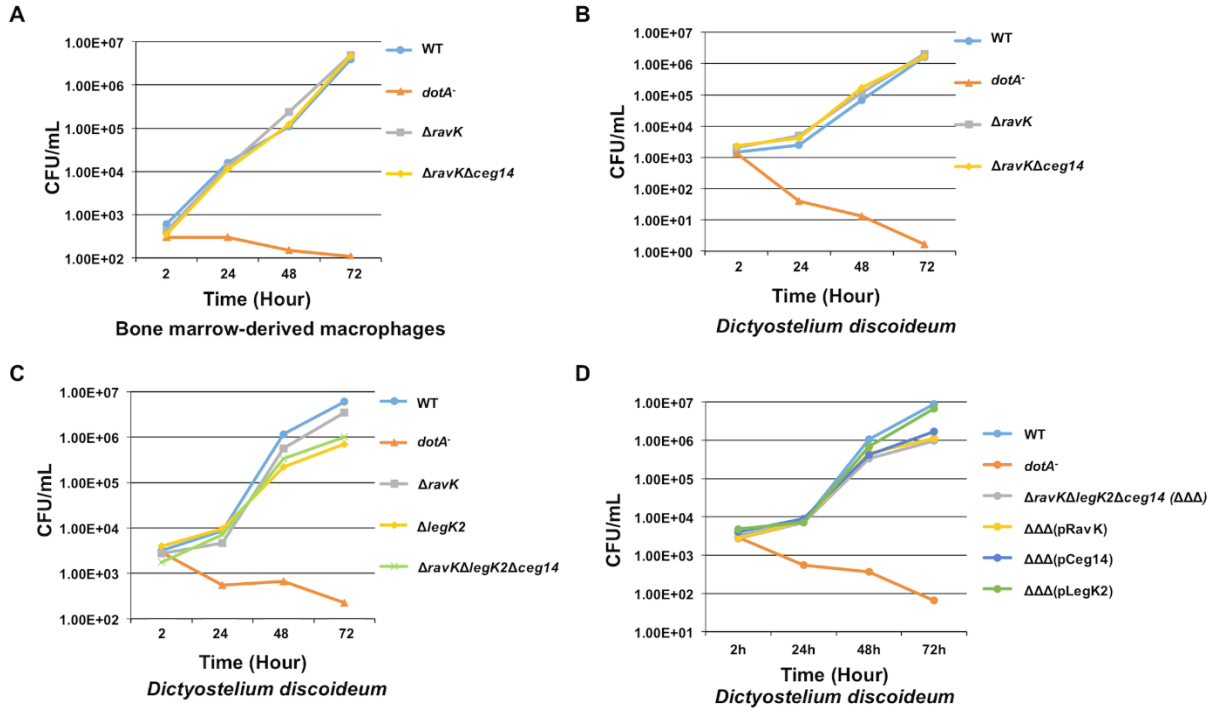


**Fig. 2-15 Deletion of ravK did not affect intracellular growth of *L. pneumophila*.**
A mutant lacking *ravK* or a mutant lacking both *ravK* and *ceg14* did not show any defects in intracellular growth in primary bone marrow-derived macrophages from A/J mice **(A)** or *D. discoideum* **(B)**. **C.** A mutant lacking *ravK*, *ceg14* and *legK2* did not show a more severe defect in intracellular growth than the *legK2* deletion mutant in *D. discoideum*. The growth defect of the triple mutant lacking *ravK*, *ceg14* and *legK2* can be complemented by *legK2* but not by *ceg14* or *ravK*. In each case, the host cells were challenged with the indicated bacterial strains grown to post-exponential phase and the total bacterial counts at the indicated time points were determined by plating appropriate dilutions of lysates onto bacteriological media to determine the CFU. Results shown are from one representative experiment done in triplicate. Similar results were obtained in three independent experiments.

## Discussion

The actin cytoskeleton is a common target exploited by many bacterial pathogens, both intra- and extracellular. Generally, bacterial effectors identified to date modulate host actin cytoskeleton by two different mechanisms of action. First, many bacterial effectors interfere with endogenous actin regulation pathways. Examples in the group include effectors that target the small GTPases Rho, Rac and Cdc42, master regulators of the actin cytoskeleton, by either distinct post-translational modifications (Just, Selzer et al., 1995, Schmidt, Sehr et al., 1997, Shao, Merritt et al., 2002, Worby, Mattoo et al., 2009, Yarbrough, Li et al., 2009), or the regulation of their GTP binding status (Fu & Galan, 1999, Goehring, Schmidt et al., 1999, Hardt, Chen et al., 1998). The second mechanism of action is to directly modify the actin molecule by means of posttranslational modifications such as ADP-ribosylation, or by crosslinking or proteolysis. ADP-ribosylation of actin leads to either promotion or inhibition of actin polymerization depending on the residues being modified. ADP-ribosylation of Arg-177 by the C2 toxin from *Clostridium botulinum* inhibits actin polymerization (Aktories et al., 1986), in contrast, the same modification of Thr-148 by the Tc toxin from *Photorhabdus luminescens* promotes actin polymerization (Lang et al., 2010). Actin cross-linking proteins secreted by *Vibrio* and *Aeromonas* species induce the production of actin oligomers that strongly inhibit Formin-mediated actin polymerization (Heisler, Kudryashova et al., 2015). Proteolysis of actin by bacterial proteins has also been documented; the metalloprotease ECP32 from *Serratia grimesii* cleaves actin, and ectopic expression of this protein enables nonpathogenic *E. coli* to invade eukaryotic cells (Bozhokina et al., 2011). In this study, we have shown that the *Legionella* Dot/Icm substrate RavK is a zinc-dependent metalloprotease that specifically cleaves actin to disrupt the actin cytoskeleton of host cells. Unlike ECP32 from *Serratia*, RavK does not affect the uptake of bacteria (**Fig. 2-15, A-B)**. Instead, RavK is likely to play a role in the replicative phase of *L. pneumophila* during infection, which is supported by the high level expression of *ravK* at the exponential growth phases in bacteriological medium (**Fig. 2-3, A-B**).

The activity of RavK toward actin generates products that can be further degraded in the cell, thereby causing the reduction of total actin levels (**Fig. 2-6, A-C**), which may explain our inability to detect cleaved actin during *L. pneumophila* infection. RavK is able to cleave purified actin in reactions free of other proteins, indicating that the cleavage of actin by RavK does not require additional proteins from the host or *L. pneumophila* (**Fig. 2-6, D**). Interestingly, RavK

exhibits a preference for non-muscle (85% β-actin and 15% γ-actin) over muscle actin (α-actin). The primary sequences of the three actin isoforms near the cleavage site are identical (**Fig. 2-11, B**), suggesting that the conformation of these actin isoforms at the cleavage site may vary, causing differences in the accessibility for the enzyme and differences in the cleavage efficiency. These results are in line with the fact that natural protozoan hosts of *L. pneumophila* such as *D. discoideum*, contain actin which shares a higher level identity of amino acid composition with human β-actin (93%) and γ-actin (93%) than with α-actin (89%).

Actin is a 375-amino acid polypeptide, which folds into two major domains. The two domains are separated by a deep cleft, in which relatively few interactions occur between the two domains. The polypeptide crosses the cleft twice in the middle of the cleft, dividing the cleft into two parts - upper and lower. The upper cleft is responsible for nucleotide binding, whereas the lower cleft is important for the interaction between actin subunits within the actin filaments. The lower cleft is lined by 11 predominantly hydrophobic residues including Leu349, Thr351(Dominguez & Holmes, 2011). Of note is that RavK cleaves actin at a site between Thr351 and Phec352, which locates on the outside end of the lower cleft, suggesting that cleavage of actin by RavK may interfere with the interaction between actin subunits in the filament and therefore inhibits the G-actin/F-actin transition. In agreement with this notion, in both the sedimentation and the pyrene-labeled actin nucleation assay, cleaved actin is defective in forming actin filaments (**Fig. 2-14, A-D**).

During *L. pneumophila* infection, translocated RavK cleaves Flag-tagged actin into a smaller form (**Fig. 2-10, A**), the size difference between the full-length and cleaved actin is similar to that observed in *in vitro* cleavage assay (**Fig. 2-6, D; Fig. 2-10, D**), indicating that RavK likely cleaves actin in the same way under these conditions. Even though we can observe a clear cleaved Flag-tagged actin during the infection of *ΔravK* strain overexpressing RavK, we were unable to detect a reduction in endogenous actin during infection (**Fig. 2-10, D**). Considering that only a small proportion of Flag-tagged actin is cleaved during infection (**Fig. 2-10, A**), and the fact that actin is very abundant in the cell, it is possible that the reduction of endogenous actin is too minute to be detected by the immunoblotting-based method. It is also possible that the host cell has a compensatory mechanism that once actin cytoskeleton is impaired due to a reduction of actin level, more actin will be synthesized to maintain the integrity of the actin cytoskeleton.

At least three *Legionella* Dot/Icm substrates have been shown to modulate the activity of components of the actin cytoskeleton. VipA is an actin nucleator, which localizes to actin rich regions and endosomes and interferes with the Multivesicular Body (MVB) pathway (Franco et al., 2012); Ceg14 is a cytosolic protein, which inhibits actin polymerization by an unknown mechanism (Guo et al., 2014a); whereas LegK2 is a kinase, which localizes to the LCV and phosphorylates two subunits of the Arp2/3 complex to inhibit actin polymerization on the LCV (Michard et al., 2015). Our demonstration of RavK as an effector that targets the actin cytoskeleton by cleaving actin indicates that *L. pneumophila* modulates this important host cellular component by diverse mechanisms. Given the essential role of actin in cellular processes, it is tempting to speculate that RavK targets to specific organelles such as the LCV, where it locally affects the function of actin in concert with effectors such as LegK2 to promote the biogenesis of the LCV. Unfortunately, we were unable to examine this hypothesis by directly staining for RavK during *L. pneumophila* infection due to low abundance of translocated RavK. Alternatively, translocated RavK may be quickly targeted for degradation by host proteases. Nevertheless, the low abundance of translocated RavK is consistent with its activity against an essential host protein. The distinct effects of multiple effectors on the actin cytoskeleton suggest the necessity of a coordinated modulation of the actin cytoskeleton at different levels. Whether these effectors directly balance the effects conferred by one or the other remains to be determined. Alternatively, given their different localization within the cell, it is plausible that these effectors regulate the actin cytoskeleton in an organelle-specific manner during *L. pneumophila* infection.

The fact that the *ravK/ceg14/legK2* triple mutant (Δ3) only has a relatively small growth defect in *D. discoideum* suggests the presence of additional Dot/Icm substrates targeting actin cytoskeleton, reiterating a significant functional redundancy among Dot/Icm substrates (O'Connor, Boyd et al., 2012). The lack of a discernible phenotype in the cell biological events associated with *L. pneumophila* infection (Finsel & Hilbi, 2015, Xu & Luo, 2013) makes it difficult to determine the benefit of targeting the actin cytoskeleton by the pathogen under current experimental conditions. Further studies are warranted to identify additional effectors that target the actin cytoskeleton and to elucidate their mechanisms of action.

# CHAPTER 3. MATERIALS AND METHODS

## Bacterial, yeast strains and plasmid construction

Bacteria strains used in this study were listed in **Table. 1**. *E. coli* strains were grown in Luria broth (LB) medium and was supplemented with antibiotics when necessary. The *L. pneumophila* strains used in this study were derivatives of the Philadelphia-1 strain Lp02 (Berger & Isberg, 1993). *L. pneumophila* was grown and maintained in CYE medium according to a standard procedure (Conover, Derre et al., 2003). The *ravK*, *ceg14* and *legK2* in-frame deletion mutants were constructed as described (Xu, Shen et al., 2010a). Briefly, for the construction of each knock-out plasmid, two pairs of primers were designed so that the target gene was replaced by 32 amino acids including the first and last 15 residues encoded by the gene and 2 residues encoded by the recognition site of *Bam*HI. For complementation experiments, the gene was expressed on the RSF1010-derived plasmid pZL507 (Xu et al., 2010a). For expression in mammalian cells, *ravK* or each of these genes was inserted into pEGFP-C1 (Clontech) or pFlag-CMV (Sigma). All the plasmids used in this study are listed in **Table. 2** and the sequences of all primers are in **Table. 3**.

## Yeast manipulation

Yeast strains used in this study were W303 (Fan, Cheng et al., 1996) and its derivatives (Table S1). Yeast strains were grown in yeast extract, peptone, dextrose medium (YPD) medium or appropriate amino acid dropout minimal media at 30°C (Tan et al., 2011). Yeast transformation was performed with the lithium acetate method (Gietz, Schiestl et al., 1995). Yeast cell lysates for protein analysis were prepared as described (Xu et al., 2010a).

## Yeast growth arrest assay

The ORF of *ravK* or its derivatives was inserted to pSB157 (Tan & Luo, 2011a) to generate pGal::*ravK* (or pGal::*ravK* derivatives), which were digested with *Stu*I and transformed into yeast strain W303. To determine the yeast growth arrest induced by the *L. pneumophila* effector, overnight cultures of relevant yeast strains grown in liquid selective medium containing glucose were serially diluted 5-fold, and 8μL of each dilution was spotted onto solid medium containing galactose or glucose. Plates were incubated at 30°C for 3 days before images were acquired.

## Tissue Culture and transfection

COS-1, and HEK293T cells were obtained from the American Type Culture Collection (Rockville, MD) and were cultured in Dulbecco's modified minimum Eagle's medium (DMEM) supplemented with 10% FBS fetal bovine/calf serum (FBS). Bone marrow-derived macrophages were prepared from A/J mice following the standard protocol (Swanson & Isberg, 1995). For transient expression of exogenous proteins in HEK293T cells, 5 µL Lipofectamine 2000 (Invitrogen) was used to introduce 2.5 µg plasmids into mammalian cells per 6-well plate well at a cell confluency of 80%. For transient expression of exogenous proteins in COS-1 cells and HEK293 cells, 5 µL Lipofectamine 3000 and 5 µL P3000 (Invitrogen) were used to introduce 2.5 µg plasmids into cells per 6-well plate well at a cell confluency of 80%.

## Protein expression and purification

To purify recombinant proteins, the appropriate gene fragments were inserted into the pQE30 plasmid (Qiagen) respectively. For protein production, 20-mL overnight culture of *E. coli* XL1blue harboring appropriate plasmid were diluted into 800 mL LB medium (100 µg/mL ampicillin) and were allowed to grow at 37°C to $OD_{600}$=0.6-0.8. After the IPTG was added to a concentration of 0.1 mM, the cultures were induced at 18°C for 16-18 h for protein expression. Bacterial cells were collected by centrifugation at 6,000*g* for 5 min and were lysed by sonication in the presence of protease inhibitors and 0.2% (wt/vol) TritonX-100. The soluble fractions were collected by centrifugation at 12,000*g* for 20 min and were incubated with Ni-NTA beads at 4°C for 2 h. Proteins bound to $Ni^{2+}$-NTA beads were washed with 20 mM imidazole and eluted with 300 mM imidazole. To remove imidazole, eluted proteins were dialyzed twice in 50 mM Tris·HCl (pH 8.0), 50 mM NaCl, 5% (vol/vol) glycerol and 1 mM DTT.

## Antibodies and Immunoblotting

Polyclonal antibodies against RavK was generated at the Pocono Rabbit Farm and Laboratory using recombinant $His_6$-tagged RavKΔC50 purified from *E. coli* to immunize rabbits respectively. The antibody was affinity purified following a standard protocol (Hubber et al., 2014a). The α-actin antibody C4 was purchased from MP Biochemicals (0869100) and was used at 1:5,000. The α-ICDH, α-GFP, α-PGK, α-Flag, α-tubulin were used as described in an earlier

study (Xu et al., 2010a). Signals from each individual protein were detected by fluorescence dye-conjugated antibodies on an Odyssey detection system (Li-Cor).

### *In vitro* cleavage assay

Rabbit skeletal muscle actin (>99% pure) (Cytoskeleton) or Human platelet non-muscle actin (>99% pure) (Cytoskeleton) were incubated with RavKΔC50 or $RavK_{H95A}$ΔC50 in G-actin buffer (5 mM Tris-HCl 8.0, 0.2 mM $CaCl_2$, 0.2 mM ATP, 0.5 mM DTT) at 22°C for indicated time periods. Protein mixtures were analyzed by SDS-PAGE followed by Coomassie brilliant blue staining.

### Determination of the metal ion requirements of RavK

To obtain metal ion-free RavKΔ50, the protein was treated by 1 mM metal ion chelator 1,10-phenanthroline at 25°C for 20 min. After treatment, each of the seven different metal ions was added into an *in vitro* actin cleavage reaction containing 5 µg actin and 0.5 µg metal ion-free RavKΔC50 at a final concentration of 0.1 mM. *In vitro* reactions were allowed to proceed for 2 h before analysis by SDS-PAGE and Coomassie brilliant blue staining.

### Determination of the cleavage site by mass spectrometry

Actin that has been incubated with RavKΔC50 was separated by SDS-PAGE and the bands corresponding to the full-length actin and its cleavage products were excised and digested with trypsin. Peptides were analyzed in an Ekspert nanoLC system 400 (Eksigent) coupled to a 5600 TripleTOF mass spectrometer (AB Sciex). Peptides were separated in a capillary C18 column (75 µm x 15 cm, ChromXP C18-CL, 3 µm, 120 Å) with the following gradient: 1 min in 5% solvent B (Solvent A: 0.1% FA and solvent B: 80% ACN/ 0.1% FA), 5-35% solvent B in 60 min, 35-80% solvent B in 1 min, 6 min in 80% solvent B, 80-5% B in 1 min, and hold in 5% for 11 min. The flow rate was set at 200 nL/min and eluting peptides were directly analyzed in the mass spectrometer. Full-MS spectra were collected in the range of 400 to 2000 m/z and the top 50 most intense parent ions were submitted to fragmentation for 50 milliseconds using rolling-collision energy. Peptides with poor MS/MS spectra were targeted to data-independent acquisition, which enabled collecting high quality spectra. MS/MS spectra searched against the human SwissProt database (downloaded on July 09, 2013) using Paragon tool of Protein Pilot software (AB Sciex)

considering biological post-translational modifications and matching peptides were inspected manually.

### Actin sedimentation and polymerization assay

30-μg G-actin was treated with 3-μg RavKΔC50, $RavK_{H95A}$ΔC50 or left untreated in G-actin buffer at RT for 2 h. The obtained actin mixtures were precleared by centrifugation at 100,000*g* for 30 min and were used in actin co-sedimentation assays following an established protocol (Namba et al., 1992). Briefly, the polymerization was initiated by adding 10× actin polymerization buffer (500 mM KCl, 10 mM $MgCl_2$, 10 mM EGTA, 10 mM ATP) and was allowed to proceed for 60 min. The samples were subjected to ultracentrifugation at 100,000*g* for 40 min. Supernatants and pellets were analyzed by SDS-PAGE, followed by Coomassie brilliant blue staining. Pyrene-actin polymerization assay was performed as described by Schafer et al with minor modifications (Schafer, Jennings et al., 1996). 60-μg non-muscle actin was treated by either $His_6$-RavKΔC50, $His_6$-$RavK_{H95A}$ΔC50 or left untreated at RT for 2 h. $His_6$-RavKΔC50, $His_6$-$RavK_{H95A}$ΔC50 were further removed from the cleaved products by passing through a $Ni^{2+}$-NTA column. The flow-through was collected and precleared by centrifugation at 100,000*g* for 30 min. 2.7 μM precleared differentially-treated actin and 0.3 μM pyrene-labeled actin were mixed. Upon the addition of 10× polymerization buffer (500 mM KCl, 10 mM $MgCl_2$, 10 mM EGTA, 100 mM imidazole HCl, pH 7.0), actin polymerization was monitored by measuring pyrene fluorescence intensity at 1s interval, using a PTI Alphascan spectrofluorimeter (Photon Technology International, South Brunswick, NJ). The excitation and emission wavelengths were set at 365 nm and 407 nm, respectively. Data were collected and processed in Excel (Microsoft) and the graph was made with Kaleidograph.

### Immunoprecipitation and *in vitro* cleavage

16-24 h after transfection, HEK293T or COS-1 cells were collected and lysed as previously described (Xu et al., 2010a). Approximately 1mg protein (in approximately 1 mL) was used for immunoprecipitation by adding 20 μL agarose beads coated with anti-Flag M2 antibody (Sigma). After incubating at 4°C for 3 h on a rotary shaker, the beads were washed with cold TBS for 4 times and proteins bound to the beads were eluted with 3×Flag peptides following manufacturer's instructions. The eluted proteins were treated with 1 μg RavKΔC50 or $RavK_{H95A}$ΔC50 in 50 μL

G-actin buffer at 22°C for 2 h. The protein mixtures were resolved with SDS-PAGE gel, and detected by the M2 antibody. Immunoprecipitation with yeast lysates was carried out as described (Xu et al., 2010a).

### Screening of *L. pneumophila* proteins that alter actin cytoskeleton

$5\times10^4$ COS-1 cells were seeded on 24-well plates and were allowed to grow at 37°C overnight. The next day, plasmids carrying full-length hypothetical *L. pneumophila* genes were introduced into COS-1 cells by Lipofectamine3000. 24 h later, cells were fixed in 4% paraformaldehyde in PBS at 25°C for 15 min, permeabilized with 0.2% Triton X-100 for 5 min, stained with Texas-red-conjugated phalloidin (1:500) at 25°C for 30 min, and subjected to imaging analysis. *L. pneumophila* genes that significantly altered the F-actin patterns of COS-1 cells were subjected to further analysis.

### F-actin and the average spread cell area quantitation

Fixed cells stained with Texas-red-conjugated phalloidin were subjected to imaging analysis under an Olympus X-81 fluorescence microscope. Images were acquired from a CoolSNAP HQ2 14-bit CCD camera (Photometrics) with identical parameters, and were similarly processed using the IPlab (BD Biosciences) and CellSens (Olympus Life Science) software package. We quantified the relative F-actin level following an established protocol (Rotty, Wu et al., 2015). Briefly, processed images were imported into ImageJ, and background was subtracted from each image. We then carefully outlined each cell by hand, and measured the integrated pixel density of each cell, which generated the average F-actin content per cell. We also measured the area occupied by each cell, which was shown as the average spread cell area.

### Intracellular bacterial growth assays

For infection experiments, *L. pneumophila* strains were grown to the post-exponential phase as measured by optical density of the culture ($OD_{600}$=3.3-3.8) and judged by an increase in bacterial motility. For *L. pneumophila* intracellular growth assay, $4\times10^5$ bone marrow-derived mouse macrophages or $5\times10^5$ *D. discoideum* were seeded on 24-well plates and were infected with relevant *L. pneumophila* strains at an MOI=0.05 at 37°C (for macrophage) or MOI=0.1 at 25°C (for *D. discoideum*). At the indicated time points, cells were treated with 0.02% saponin for half

an hour and the bacteria number was determined by enumerating colony-forming unit (CFU) of appropriately diluted saponin-soluble fractions.

### Determination of the cleavage of actin during infection

HEK293 cells were transfected to express 4×Flag-Actin and FCγRII (Kagan & Roy, 2002b) for 24 h with Lipofectamine 3000 (Life Technology). Bacteria of relevant *L. pneumophila* strains were opsonized with rabbit anti-*Legionella* antibodies (Xu et al., 2010a) at 1:500 for 30 min before infecting the cells at an MOI of 50 for 2 h. Cleared lysates prepared from infected cells were subjected to immunoblotting with M2 antibody (Sigma). For experiments to determine the endogenous actin level during infection, HEK293 cells were transfected to express FCγRII (Kagan & Roy, 2002b) for 24 h with Lipofectamine 3000 (Life Technology), bacterial infections were performed as described above. Cleared lysates prepared from infected cells were probed by immunoblotting with an actin-specific antibody.

### Determination of RavK translocation by *L. pneumophila*

HEK293 cells were transfected to express FCγRII for 24 h with Lipofectamine 3000 (Life Technology). Bacteria of relevant *L. pneumophila* strains were opsonized with rabbit anti-*Legionella* antibodies (Xu et al., 2010a) at 1:500 for 30 min before infecting the cells at an MOI of 50 for 2 h. Infected cells were lysed with 0.02% saponin, which lyses membranes of mammalian cells but not of bacterial cells. The lysates were probed for RavK with a specific antibody. Translocation of the effector SidC (Luo & Isberg, 2004) was probed as a control.

### Data quantitation and statistical analyses

Immunoblots were scanned with the Odyssey 3.0 (LI-COR Biosciences) and quantified with ImageJ. Statistical significance for all relevant data was calculated using the unpaired two-tailed Student *t* tests, with a $p$ value $<0.05$ being considered as significant difference.

# APPENDIX

**Table. 1 Bacterial and yeast strains used in this study**

| Strains | Genotype, relevant markers | Reference |
|---|---|---|
| *E. coli* | | |
| XL1-Blue | *recA1* endA1 *gyrA*96 *thi-1 hsd*R17 *sup*E44 *relA*1 *lac* [*F'* *proAB lacI*$^{q}$*ZM15* Tn*10*(Tet$^{r}$)] | Stratagene |
| DH5α(λpir) | supE44 d*lacU169*(φ80*lacZ*Δ*M15*) *hsdR17 recA1 endA1 gyrA96 thi-1 relA1 pir tet*::*Mu recA* | Our collection |
| *L. pneumophila* | | |
| Lp02 | Philadelphia-1 *rpsL hsdR thyA* | (Berger & Isberg, 1993) |
| Lp03 | Lp02(*dotA*$^{-}$) | (Berger & Isberg, 1993) |
| Lp02(pJB908) | Lp02(pJB908) | (Liu & Luo, 2007) |
| Lp03(pJB908) | Lp03(pJB908) | (Liu & Luo, 2007) |
| ZL1101 | Lp02Δ*ravK* | This study |
| ZL1102 | Lp02Δ*ravK* (pJB908) | This study |
| ZL1103 | Lp02Δ*ravK* (pZL507::*ravK*) | This study |
| ZL1104 | Lp02Δ*ravK*Δ*ceg14* | This study |
| ZL1105 | Lp02Δ*ravK*Δ*ceg14* (pJB908) | This study |
| ZL1106 | Lp02Δ*ravK*Δ*ceg14*Δ*legK2* | This study |
| ZL1107 | Lp02Δ*ravK*Δ*ceg14*Δ*legK2* (pJB908) | This study |
| ZL1108 | Lp02Δ*ravK*Δ*ceg14*Δ*legK2* (pZL507::*ravK*) | This study |
| ZL1109 | Lp02Δ*ravK*Δ*ceg14*Δ*legK2* (pZL507::*ceg14*) | This study |
| ZL1110 | Lp02Δ*ravK*Δ*ceg14*Δ*legK2* (pZL507::*legK2*) | This study |
| Yeast | | |
| W303 | *MATa/MAT α [leu2-3,112 trp1-1 can1-100 ura3-1 ade2-1 his3-11,15] [phi+]* | (Fan et al., 1996) |

**Table. 2 Plasmids used in this study**

| Plasmid | Relevant phenotypes | Sources |
|---|---|---|
| pSR47s | *ori*R6K, *ori*T RP4, $Kan^R$, *SacB* | (Dumenil & Isberg, 2001) |
| pQE30 | Amp | Qiagen |
| pJB908 | Amp, $thy^+$ | (Bardill et al., 2005) |
| pZL507 | For expression $His_6$-tagged protein *L. pneumophila* | (Xu et al., 2010a) |
| pEGFPC-1 | For expressing C-terminal GFP fusion proteins | Clontech |
| pYES/NT A | Yeast expression vector with N-terminal tag | Invitrogen |
| pSB157m | Amp, $ura^+$, GAL promoter | (Tan & Luo, 2011b) |
| p415-ADH | Amp, $leu^+$, ADH promoter | (Mumberg, Muller et al., 1995) |
| pZLΔ*ravK* | Construct used for in-frame deletion of *ravK* | This study |
| pZLΔ*ceg14* | Construct used for in-frame deletion of *ceg14* | (Guo et al., 2014a) |
| pZLΔ*legK2* | Construct used for in-frame deletion of *legK2* | This study |
| pZL1201 | pYES/NT A::*ravK* | This study |
| pZL1202 | pYES/NT A::$ravK_{H95A}$ | This study |
| pZL1203 | pYES/NT A::$ravK_{E96A}$ | This study |
| pZL1204 | pYES/NT A::$ravK_{H99A}$ | This study |
| pZL1205 | pEGFPc1::*lpg0483* | This study |
| pZL1206 | pEGFPc1::*lpg0944*(*ravJ*) | This study |
| pZL1207 | pEGFPc1::*lpg1290* | This study |
| pZL1208 | pEGFPc1::*lpg1798* | This study |
| pZL1209 | pEGFPc1::*lpg1961* | This study |
| pZL1210 | pEGFPc1::*lpg2322* | This study |
| pZL1211 | pEGFPc1::*lpg2603* | This study |
| pZL1212 | pEGFPc1::*ravK* | This study |
| pZL1213 | pEGFPc1::$ravK_{H95A}$ | This study |
| pZL1214 | pEGFPc1::$ravK_{E96A}$ | This study |
| pZL1215 | pEGFPc1::$ravK_{E96A}$ | This study |

Table. 2 continued

| | | |
|---|---|---|
| pZL1216 | pEGFPc1::*ravK*ΔC50 | This study |
| pZL1217 | pSB157m::*ravK* | This study |
| pZL1218 | pSB157m::*ravK*ΔC50 | This study |
| pZL1219 | pSB157m::*ravK*ΔC50$_{H95A}$ | This study |
| pZL1220 | pSB157m::*ravK*ΔC100 | This study |
| pZL1221 | pQE30::*ravK*ΔC50 | This study |
| pZL1222 | pQE30::*ravK*ΔC50$_{H95A}$ | This study |
| pZL1223 | pCMV-1XFlag-β-actin | This study |
| pZL1224 | pCMV-1XFlag-β-actin$_{L349A}$ | This study |
| pZL1225 | pCMV-1XFlag-β-actin$_{S350A}$ | This study |
| pZL1226 | pCMV-1XFlag-β-actin$_{T351A}$ | This study |
| pZL1227 | pCMV-1XFlag-β-actin$_{F352A}$ | This study |
| pZL1228 | pCMV-1XFlag-β-actin$_{Q353A}$ | This study |
| pZL1229 | pCMV-1XFlag-β-actin$_{Q354A}$ | This study |
| pZL1234 | p415ADH | (Mumberg et al., 1995) |

**Table. 3 Primers used in this study**

| Primer | Sequence (Restriction enzyme sites are underlined) | Note |
|---|---|---|
| PL1101 | CTGGGATCCATGGTAAGTTTGGAGCAT | ravK5'BamHI |
| PL1102 | CTGGTCGACTTATATATCAAGCTTTAT | ravK3'SalI |
| PL1103 | CTGAAGCTTATGGATGATGATATCGCCGC | β-actin5'HindIII |
| PL1104 | CTGCTCGAGCTAGAAGCATTTGCGGTGGA | β-actin3'XhoI |
| PL1105 | ATACTCGAGAAATGCCATGCTTAATAA | ravK up XhoI knockout |
| PL1106 | ATAGGATCCCCTACATTCCGAAATAAG | ravK up BamHI knockout |
| PL1107 | ATAGGATCCGAGCATTTTCATTCTCCT | ravK down BamHI knockout |
| PL1108 | ATAGCGGCCGCATAATGGAATTGTTTACT | ravK down NotI knockout |
| PL1109 | CTGGTCGACTAATCGTTTATGATAGTAAA | legK2 up SalI knock-out |
| PL1110 | CTGGGATCCATCTTGATGTAAAGGTTGTT | legK2 up BamHI knockout |
| PL1111 | CTGGGATCCAAGCAACCTATATTTACCCC | legK2 down BamHI knockout |
| PL1112 | CTGGAGCTCATTTTATCCTGCTGAATACC | legK2 down SacI knockout |
| PL1113 | TTAAAAGCATGACCAGTTTCAGCAACAAT AGCACCAATAATTTTGATCGCC | ravK(H95A)-1 |
| PL1114 | GGCGATCAAAATTATTGGTGCTATTGTTGC TGAAACTGGTCATGCTTTTAA | ravK(H95A)-2 |
| PL1115 | CCACATTAAAAGCATGACCAGTTGCATGAA CAATAGCACCAATAATT | ravK(E96A)-1 |
| PL1116 | AATTATTGGTGCTATTGTTCATGCAACTGGT CATGCTTTTAATGTGG | ravK(E96A)-2 |
| PL1117 | CAGCCACATTAAAAGCAGCACCAGTTTCAT GAACAATAGCACCAA | ravK(H99A)-1 |
| PL1118 | TTGGTGCTATTGTTCATGAAACTGGTGCTGC TTTTAATGTGGCTG | ravK(H99A)-2 |
| PL1119 | GCTGGAAGGTGGACGACGAGGCCAGGATGG | β-actin(L349S)-1 |
| PL1120 | CCATCCTGGCCTCGTCGTCCACCTTCCAGC | β-actin(L349S)-1 |

Table. 3 continued

| | | |
|---|---|---|
| PL1121 | GCTGGAAGGTGGCCAGCGAGGCCAG | β-actin(S350A)-1 |
| PL1122 | CTGGCCTCGCTGGCCACCTTCCAGC | β-actin(S350A)-1 |
| PL1123 | ATCTGCTGGAAGGCGGACAGCGAGGCC | β-actin(T351A)-1 |
| PL1124 | GGCCTCGCTGTCCGCCTTCCAGCAGAT | β-actin(T351A)-1 |
| PL1125 | ATCCACATCTGCTGGGCGGTGGACAGCGAGGC | β-actin(F352A)-1 |
| PL1126 | GCCTCGCTGTCCACCGCCCAGCAGATGTGGAT | β-actin(F352A)-2 |
| PL1127 | CTCGCTGTCCACCTTCGCGCAGATGTGGATCAGC | β-actin(Q353A)-1 |
| PL1128 | GCTGATCCACATCTGCGCGAAGGTGGACAGCGAG | β-actin(Q353A)-1 |
| PL1129 | CTTGCTGATCCACATCGCCTGGAAGGTGGACAGC | β-actin(Q354A)-1 |
| PL1130 | GCTGTCCACCTTCCAGGCGATGTGGATCAGCAAG | β-actin(Q354A)-1 |

# REFERENCES


Aktories K, Barmann M, Ohishi I, Tsuyama S, Jakobs KH, Habermann E (1986) Botulinum C2 toxin ADP-ribosylates actin. Nature 322: 390-2

Allaire PD, Marat AL, Dall'Armi C, Di Paolo G, McPherson PS, Ritter B (2010) The Connecdenn DENN domain: a GEF for Rab35 mediating cargo-specific exit from early endosomes. Mol Cell 37: 370-82

Altman E, Segal G (2008) The response regulator CpxR directly regulates expression of several Legionella pneumophila icm/dot components as well as new translocated substrates. Journal of Bacteriology 190: 1985-1996

Arasaki K, Kimura H, Tagaya M, Roy CR (2018) Legionella remodels the plasma membrane-derived vacuole by utilizing exocyst components as tethers. J Cell Biol

Arasaki K, Roy CR (2010) Legionella pneumophila Promotes Functional Interactions between Plasma Membrane Syntaxins and Sec22b. Traffic 11: 587-600

Arasaki K, Toomre DK, Roy CR (2012) The Legionella pneumophila Effector DrrA Is Sufficient to Stimulate SNARE-Dependent Membrane Fusion. Cell Host & Microbe 11: 46-57

Bardill JP, Miller JL, Vogel JP (2005) IcmS-dependent translocation of SdeA into macrophages by the Legionella pneumophila type IV secretion system. Mol Microbiol 56: 90-103

Barlocher K, Hutter CAJ, Swart AL, Steiner B, Welin A, Hohl M, Letourneur F, Seeger MA, Hilbi H (2017) Structural insights into Legionella RidL-Vps29 retromer subunit interaction reveal displacement of the regulator TBC1D5. Nat Commun 8

Berger KH, Isberg RR (1993) Two distinct defects in intracellular growth complemented by a single genetic locus in Legionella pneumophila. Mol Microbiol 7: 7-19

Berger KH, Merriam JJ, Isberg RR (1994) Altered intracellular targeting properties associated with mutations in the Legionella pneumophila dotA gene. Mol Microbiol 14: 809-22

Bhogaraju S, Kalayil S, Liu Y, Bonn F, Colby T, Matic I, Dikic I (2016) Phosphoribosylation of Ubiquitin Promotes Serine Ubiquitination and Impairs Conventional Ubiquitination. Cell 167: 1636-1649 e13

Bock CW, Katz AK, Markham GD, Glusker JP (1999) Manganese as a replacement for magnesium and zinc: Functional comparison of the divalent ions. J Am Chem Soc 121: 7360-7372

Bonifacino JS, Hurley JH (2008) Retromer. Curr Opin Cell Biol 20: 427-36

Bozhokina ES, Tsaplina OA, Efremova TN, Kever LV, Demidyukt IV, Kostrov SV, Adam T, Komissarchik VY, Khaitlina SY (2011) Bacterial invasion of eukaryotic cells can be mediated by actin-hydrolysing metalloproteases grimelysin and protealysin. Cell Biol Int 35: 111-118

Brand BC, Sadosky AB, Shuman HA (1994) The Legionella pneumophila icm locus: a set of genes required for intracellular multiplication in human macrophages. Mol Microbiol 14: 797-808

Brombacher E, Urwyler S, Ragaz C, Weber SS, Kami K, Overduin M, Hilbi H (2009) Rab1 guanine nucleotide exchange factor SidM is a major phosphatidylinositol 4-phosphate-binding effector protein of Legionella pneumophila. J Biol Chem 284: 4846-56

Burstein D, Amaro F, Zusman T, Lifshitz Z, Cohen O, Gilbert JA, Pupko T, Shuman HA, Segal G (2016) Genomic analysis of 38 Legionella species identifies large and diverse effector repertoires. Nat Genet 48: 167-75

Burstein D, Zusman T, Degtyar E, Viner R, Segal G, Pupko T (2009) Genome-scale identification of Legionella pneumophila effectors using a machine learning approach. PLoS Pathog 5: e1000508

Cambronne ED, Roy CR (2007) The Legionella pneumophila IcmSW complex interacts with multiple Dot/Icm effectors to facilitate type IV translocation. PLoS Pathog 3: e188

Campodonico EM, Chesnel L, Roy CR (2005) A yeast genetic system for the identification and characterization of substrate proteins transferred into host cells by the Legionella pneumophila Dot/lcm system. Molecular Microbiology 56: 918-933

Chen J, de Felipe KS, Clarke M, Lu H, Anderson OR, Segal G, Shuman HA (2004) Legionella effectors that promote nonlytic release from protozoa. Science 303: 1358-1361

Chetrit D, Hu B, Christie PJ, Roy CR, Liu J (2018) A unique cytoplasmic ATPase complex defines the Legionella pneumophila type IV secretion channel. Nat Microbiol 3: 678-686

Chisholm ST, Dahlbeck D, Krishnamurthy N, Day B, Sjolander K, Staskawicz BJ (2005) Molecular characterization of proteolytic cleavage sites of the Pseudomonas syringae effector AvrRpt2. Proc Natl Acad Sci U S A 102: 2087-92

Conover GM, Derre I, Vogel JP, Isberg RR (2003) The Legionella pneumophila LidA protein: a translocated substrate of the Dot/Icm system associated with maintenance of bacterial integrity. Molecular Microbiology 48: 305-321

Correia AM, Ferreira JS, Borges V, Nunes A, Gomes B, Capucho R, Goncalves J, Antunes DM, Almeida S, Mendes A, Guerreiro M, Sampaio DA, Vieira L, Machado J, Simoes MJ, Goncalves P, Gomes JP (2016) Probable Person-to-Person Transmission of Legionnaires' Disease. N Engl J Med 374: 497-8

de Felipe KS, Pampou S, Jovanovic OS, Pericone CD, Ye SF, Kalachikov S, Shuman HA (2005) Evidence for acquisition of Legionella type IV secretion substrates via interdomain horizontal gene transfer. J Bacteriol 187: 7716-26

Derre I, Isberg RR (2004) Legionella pneumophila replication vacuole formation involves rapid recruitment of proteins of the early secretory system. Infect Immun 72: 3048-53

Di Paolo G, De Camilli P (2006) Phosphoinositides in cell regulation and membrane dynamics. Nature 443: 651-657

Dominguez R, Holmes KC (2011) Actin structure and function. Annual review of biophysics 40: 169-86

Dong N, Niu M, Hu L, Yao Q, Zhou R, Shao F (2016) Modulation of membrane phosphoinositide dynamics by the phosphatidylinositide 4-kinase activity of the Legionella LepB effector. Nat Microbiol 2: 16236

Dorer MS, Kirton D, Bader JS, Isberg RR (2006) RNA interference analysis of Legionella in Drosophila cells: Exploitation of early secretory apparatus dynamics. Plos Pathogens 2: 315-327

Dumenil G, Isberg RR (2001) The Legionella pneumophila IcmR protein exhibits chaperone activity for IcmQ by preventing its participation in high-molecular-weight complexes. Molecular microbiology 40: 1113-27

Ensminger AW, Isberg RR (2010) E3 ubiquitin ligase activity and targeting of BAT3 by multiple Legionella pneumophila translocated substrates. Infect Immun 78: 3905-19

Fan HY, Cheng KK, Klein HL (1996) Mutations in the RNA polymerase II transcription machinery suppress the hyperrecombination mutant hpr1 delta of Saccharomyces cerevisiae. Genetics 142: 749-59

Fasshauer D, Sutton RB, Brunger AT, Jahn R (1998) Conserved structural features of the synaptic fusion complex: SNARE proteins reclassified as Q- and R-SNAREs. P Natl Acad Sci USA 95: 15781-15786

Fields BS, Barbaree JM, Shotts EB, Feeley JC, Morrill WE, Sanden GN, Dykstra MJ (1986) Comparison of Guinea-Pig and Protozoan Models for Determining Virulence of Legionella Species. Infection and Immunity 53: 553-559

Finsel I, Hilbi H (2015) Formation of a pathogen vacuole according to Legionella pneumophila: how to kill one bird with many stones. Cell Microbiol 17: 935-50

Finsel I, Ragaz C, Hoffmann C, Harrison CF, Weber S, van Rahden VA, Johannes L, Hilbi H (2013) The Legionella effector RidL inhibits retrograde trafficking to promote intracellular replication. Cell Host Microbe 14: 38-50

Franco IS, Shohdy N, Shuman HA (2012) The Legionella pneumophila effector VipA is an actin nucleator that alters host cell organelle trafficking. PLoS Pathog 8: e1002546

Fraser DW, Tsai TR, Orenstein W, Parkin WE, Beecham HJ, Sharrar RG, Harris J, Mallison GF, Martin SM, McDade JE, Shepard CC, Brachman PS (1977) Legionnaires' disease: description of an epidemic of pneumonia. N Engl J Med 297: 1189-97

Fu Y, Galan JE (1999) A salmonella protein antagonizes Rac-1 and Cdc42 to mediate host-cell recovery after bacterial invasion. Nature 401: 293-7

Galan JE (2001) Salmonella interactions with host cells: Type III secretion at work. Annu Rev Cell Dev Bi 17: 53-86

Gaspar AH, Machner MP (2014) VipD is a Rab5-activated phospholipase A1 that protects Legionella pneumophila from endosomal fusion. Proc Natl Acad Sci U S A 111: 4560-5

Ghosal D, Chang YW, Jeong KC, Vogel JP, Jensen GJ (2017) In situ structure of the Legionella Dot/Icm type IV secretion system by electron cryotomography. EMBO Rep 18: 726-732

Gietz RD, Schiestl RH, Willems AR, Woods RA (1995) Studies on the transformation of intact yeast cells by the LiAc/SS-DNA/PEG procedure. Yeast 11: 355-60

Goehring UM, Schmidt G, Pederson KJ, Aktories K, Barbieri JT (1999) The N-terminal domain of Pseudomonas aeruginosa exoenzyme S is a GTPase-activating protein for Rho GTPases. J Biol Chem 274: 36369-72

Goody PR, Heller K, Oesterlin LK, Muller MP, Itzen A, Goody RS (2012) Reversible phosphocholination of Rab proteins by Legionella pneumophila effector proteins. Embo J 31: 1774-1784

Grosshans BL, Ortiz D, Novick P (2006) Rabs and their effectors: achieving specificity in membrane traffic. Proc Natl Acad Sci U S A 103: 11821-7

Guo Z, Stephenson R, Qiu J, Zheng S, Luo ZQ (2014a) A Legionella effector modulates host cytoskeletal structure by inhibiting actin polymerization. Microbes Infect 16: 225-36

Guo ZH, Stephenson R, Qiu JZ, Zheng SJ, Luo ZQ (2014b) A Legionella effector modulates host cytoskeletal structure by inhibiting actin polymerization. Microbes Infect 16: 225-236

Hardt WD, Chen LM, Schuebel KE, Bustelo XR, Galan JE (1998) S. typhimurium encodes an activator of Rho GTPases that induces membrane ruffling and nuclear responses in host cells. Cell 93: 815-26

Heidtman M, Chen EJ, Moy MY, Isberg RR (2009) Large-scale identification of Legionella pneumophila Dot/Icm substrates that modulate host cell vesicle trafficking pathways. Cellular Microbiology 11: 230-248

Heisler DB, Kudryashova E, Grinevich DO, Suarez C, Winkelman JD, Birukov KG, Kotha SR, Parinandi NL, Vavylonis D, Kovar DR, Kudryashov DS (2015) ACTIN-DIRECTED TOXIN. ACD toxin-produced actin oligomers poison formin-controlled actin polymerization. Science 349: 535-9

Herman IM (1993) Actin isoforms. Curr Opin Cell Biol 5: 48-55

Horenkamp FA, Mukherjee S, Alix E, Schauder CM, Hubber AM, Roy CR, Reinisch KM (2014) Legionella pneumophila Subversion of Host Vesicular Transport by SidC Effector Proteins. Traffic 15: 488-499

Horwitz MA (1987) Characterization of avirulent mutant Legionella pneumophila that survive but do not multiply within human monocytes. J Exp Med 166: 1310-28

Hsu F, Zhu W, Brennan L, Tao L, Luo ZQ, Mao Y (2012) Structural basis for substrate recognition by a unique Legionella phosphoinositide phosphatase. Proc Natl Acad Sci U S A 109: 13567-72

Hsu FS, Luo X, Qiu JZ, Teng YB, Jin JP, Smolka MB, Luo ZQ, Mao YX (2014) The Legionella effector SidC defines a unique family of ubiquitin ligases important for bacterial phagosomal remodeling. P Natl Acad Sci USA 111: 10538-10543

Huang L, Boyd D, Amyot WM, Hempstead AD, Luo ZQ, O'Connor TJ, Chen C, Machner M, Montminy T, Isberg RR (2011) The E Block motif is associated with Legionella pneumophila translocated substrates. Cell Microbiol 13: 227-45

Hubber A, Arasaki K, Nakatsu F, Hardiman C, Lambright D, De Camilli P, Nagai H, Roy CR (2014a) The machinery at endoplasmic reticulum-plasma membrane contact sites contributes to spatial regulation of multiple Legionella effector proteins. PLoS pathogens 10: e1004222

Hubber A, Kubori T, Nagai H (2014b) Modulation of the Ubiquitination Machinery by Legionella. Curr Top Microbiol 376: 227-247

Ingmundson A, Delprato A, Lambright DG, Roy CR (2007) Legionella pneumophila proteins that regulate Rab1 membrane cycling. Nature 450: 365-U1

Isberg RR, O'Connor TJ, Heidtman M (2009) The Legionella pneumophila replication vacuole: making a cosy niche inside host cells. Nature reviews Microbiology 7: 13-24

Jeong KC, Ghosal D, Chang YW, Jensen GJ, Vogel JP (2017) Polar delivery of Legionella type IV secretion system substrates is essential for virulence. Proc Natl Acad Sci U S A 114: 8077-8082

Jongeneel CV, Bouvier J, Bairoch A (1989) A unique signature identifies a family of zinc-dependent metallopeptidases. FEBS letters 242: 211-4

Just I, Selzer J, Wilm M, von Eichel-Streiber C, Mann M, Aktories K (1995) Glucosylation of Rho proteins by Clostridium difficile toxin B. Nature 375: 500-3

Kagan JC, Roy CR (2002a) Legionella phagosomes intercept vesicular traffic from endoplasmic reticulum exit sites. Nat Cell Biol 4: 945-954

Kagan JC, Roy CR (2002b) Legionella phagosomes intercept vesicular traffic from endoplasmic reticulum exit sites. Nat Cell Biol 4: 945-54

Kagan JC, Stein MP, Pypaert M, Roy CR (2004) Legionella subvert the functions of Rab1 and Sec22b to create a replicative organelle. J Exp Med 199: 1201-11

Kerscher O, Felberbaum R, Hochstrasser M (2006) Modification of proteins by ubiquitin and ubiquitin-like proteins. Annu Rev Cell Dev Bi 22: 159-180

King NP, Newton P, Schuelein R, Brown DL, Petru M, Zarsky V, Dolezal P, Luo L, Bugarcic A, Stanley AC, Murray RZ, Collins BM, Teasdale RD, Hartland EL, Stow JL (2015) Soluble NSF attachment protein receptor molecular mimicry by a Legionella pneumophilaDot/Icm effector. Cellular Microbiology 17: 767-784

Komano T, Yoshida T, Narahara K, Furuya N (2000) The transfer region of Incl1 plasmid R64: similarities between R64 tra and Legionella icm/dot genes. Molecular Microbiology 35: 1348-1359

Kotewicz KM, Ramabhadran V, Sjoblom N, Vogel JP, Haenssler E, Zhang MY, Behringer J, Scheck RA, Isberg RR (2017) A Single Legionella Effector Catalyzes a Multistep Ubiquitination Pathway to Rearrange Tubular Endoplasmic Reticulum for Replication. Cell Host & Microbe 21: 169-181

Ku B, Lee KH, Park WS, Yang CS, Ge J, Lee SG, Cha SS, Shao F, Heo WD, Jung JU, Oh BH (2012) VipD of Legionella pneumophila targets activated Rab5 and Rab22 to interfere with endosomal trafficking in macrophages. PLoS Pathog 8: e1003082

Kubori T, Hyakutake A, Nagai H (2008) Legionella translocates an E3 ubiquitin ligase that has multiple U-boxes with distinct functions. Molecular Microbiology 67: 1307-1319

Kubori T, Kitao T, Ando H, Nagai H (2018) LotA, a Legionella deubiquitinase, has dual catalytic activity and contributes to intracellular growth. Cellular Microbiology 20

Kubori T, Koike M, Bui XT, Higaki S, Aizawa S, Nagai H (2014) Native structure of a type IV secretion system core complex essential for Legionella pathogenesis. Proc Natl Acad Sci U S A 111: 11804-9

Kubori T, Shinzawa N, Kanuka H, Nagai H (2010) Legionella Metaeffector Exploits Host Proteasome to Temporally Regulate Cognate Effector. Plos Pathogens 6

Kumar Y, Valdivia RH (2008) Actin and intermediate filaments stabilize the Chlamydia trachomatis vacuole by forming dynamic structural scaffolds. Cell Host & Microbe 4: 159-169

Kuroda T, Kubori T, Thanh Bui X, Hyakutake A, Uchida Y, Imada K, Nagai H (2015) Molecular and structural analysis of Legionella DotI gives insights into an inner membrane complex essential for type IV secretion. Sci Rep 5: 10912

Kwak MJ, Kim JD, Kim H, Kim C, Bowman JW, Kim S, Joo K, Lee J, Jin KS, Kim YG, Lee NK, Jung JU, Oh BH (2017) Architecture of the type IV coupling protein complex of Legionella pneumophila. Nat Microbiol 2: 17114

Lang AE, Schmidt G, Schlosser A, Hey TD, Larrinua IM, Sheets JJ, Mannherz HG, Aktories K (2010) Photorhabdus luminescens toxins ADP-ribosylate actin and RhoA to force actin clustering. Science 327: 1139-42

Lau HY, Ashbolt NJ (2009) The role of biofilms and protozoa in Legionella pathogenesis: implications for drinking water. J Appl Microbiol 107: 368-78

Lifshitz Z, Burstein D, Peeri M, Zusman T, Schwartz K, Shuman HA, Pupko T, Segal G (2013) Computational modeling and experimental validation of the Legionella and Coxiella virulence-related type-IVB secretion signal. Proc Natl Acad Sci U S A 110: E707-15

Lin YH, Doms AG, Cheng E, Kim B, Evans TR, Machner MP (2015) Host Cell-catalyzed S-Palmitoylation Mediates Golgi Targeting of the Legionella Ubiquitin Ligase GobX. Journal of Biological Chemistry 290: 25766-25781

Lin YH, Lucas M, Evans TR, Abascal-Palacios G, Doms AG, Beauchene NA, Rojas AL, Hierro A, Machner MP (2018) RavN is a member of a previously unrecognized group of Legionella pneumophila E3 ubiquitin ligases. Plos Pathogens 14

Liu Y, Luo ZQ (2007) The Legionella pneumophila effector SidJ is required for efficient recruitment of endoplasmic reticulum proteins to the bacterial phagosome. Infect Immun 75: 592-603

Luo ZQ, Isberg RR (2004) Multiple substrates of the Legionella pneumophila Dot/Icm system identified by interbacterial protein transfer. Proc Natl Acad Sci U S A 101: 841-6

Machner MP, Isberg RR (2006) Targeting of host Rab GTPase function by the intravacuolar pathogen Legionella pneumophila. Dev Cell 11: 47-56

Machner MP, Isberg RR (2007) A bifunctional bacterial protein links GDI displacement to Rab1 activation. Science 318: 974-977

Marra A, Blander SJ, Horwitz MA, Shuman HA (1992) Identification of a Legionella pneumophila locus required for intracellular multiplication in human macrophages. Proc Natl Acad Sci U S A 89: 9607-11

Marra A, Shuman HA (1989) Isolation of a Legionella pneumophila restriction mutant with increased ability to act as a recipient in heterospecific matings. J Bacteriol 171: 2238-40

McDade JE, Shepard CC, Fraser DW, Tsai TR, Redus MA, Dowdle WR (1977) Legionnaires' disease: isolation of a bacterium and demonstration of its role in other respiratory disease. N Engl J Med 297: 1197-203

Meir A, Chetrit D, Liu L, Roy CR, Waksman G (2018) Legionella DotM structure reveals a role in effector recruiting to the Type 4B secretion system. Nat Commun 9: 507

Merriam JJ, Mathur R, Maxfield-Boumil R, Isberg RR (1997) Analysis of the Legionella pneumophila fliI gene: intracellular growth of a defined mutant defective for flagellum biosynthesis. Infect Immun 65: 2497-501

Michard C, Sperandio D, Bailo N, Pizarro-Cerda J, LeClaire L, Chadeau-Argaud E, Pombo-Gregoire I, Hervet E, Vianney A, Gilbert C, Faure M, Cossart P, Doublet P (2015) The Legionella Kinase LegK2 Targets the ARP2/3 Complex To Inhibit Actin Nucleation on Phagosomes and Allow Bacterial Evasion of the Late Endocytic Pathway. mBio 6: e00354-15

Mizuno-Yamasaki E, Rivera-Molina F, Novick P (2012) GTPase networks in membrane traffic. Annu Rev Biochem 81: 637-59

Mockrin SC, Korn ED (1980) Acanthamoeba Profilin Interacts with G-Actin to Increase the Rate of Exchange of Actin-Bound Adenosine 5'-Triphosphate. Biochemistry-Us 19: 5359-5362

Mukherjee S, Liu X, Arasaki K, McDonough J, Galan JE, Roy CR (2011) Modulation of Rab GTPase function by a protein phosphocholine transferase. Nature 477: 103-6

Muller MP, Peters H, Blumer J, Blankenfeldt W, Goody RS, Itzen A (2010) The Legionella effector protein DrrA AMPylates the membrane traffic regulator Rab1b. Science 329: 946-9

Mullins RD, Pollard TD (1999) Structure and function of the Arp2/3 complex. Curr Opin Struc Biol 9: 244-249

Mumberg D, Muller R, Funk M (1995) Yeast vectors for the controlled expression of heterologous proteins in different genetic backgrounds. Gene 156: 119-22

Murata T, Delprato A, Ingmundson A, Toomre DK, Lambright DG, Roy CR (2006) The Legionella pneumophila effector protein DrrA is a Rab1 guanine nucleotide-exchange factor. Nat Cell Biol 8: 971-U76

Nagai H, Cambronne ED, Kagan JC, Amor JC, Kahn RA, Roy CR (2005) A C-terminal translocation signal required for Dot/Icm-dependent delivery of the Legionella RalF protein to host cells. Proc Natl Acad Sci U S A 102: 826-31

Nagai H, Kagan JC, Zhu X, Kahn RA, Roy CR (2002) A bacterial guanine nucleotide exchange factor activates ARF on Legionella phagosomes. Science 295: 679-82

Nagai H, Kubori T (2011) Type IVB Secretion Systems of Legionella and Other Gram-Negative Bacteria. Front Microbiol 2: 136

Namba Y, Ito M, Zu Y, Shigesada K, Maruyama K (1992) Human T cell L-plastin bundles actin filaments in a calcium-dependent manner. Journal of biochemistry 112: 503-7

Neunuebel MR, Chen Y, Gaspar AH, Backlund PS, Yergey A, Machner MP (2011) De-AMPylation of the Small GTPase Rab1 by the Pathogen Legionella pneumophila. Science 333: 453-456

Newton HJ, Ang DK, van Driel IR, Hartland EL (2010) Molecular pathogenesis of infections caused by Legionella pneumophila. Clin Microbiol Rev 23: 274-98

Ninio S, Zuckman-Cholon DM, Cambronne ED, Roy CR (2005) The Legionella IcmS-IcmW protein complex is important for Dot/Icm-mediated protein translocation. Mol Microbiol 55: 912-26

O'Connor TJ, Boyd D, Dorer MS, Isberg RR (2012) Aggravating genetic interactions allow a solution to redundancy in a bacterial pathogen. Science 338: 1440-4

Oesterlin LK, Goody RS, Itzen A (2012) Posttranslational modifications of Rab proteins cause effective displacement of GDP dissociation inhibitor. P Natl Acad Sci USA 109: 5621-5626

Pan X, Luhrmann A, Satoh A, Laskowski-Arce MA, Roy CR (2008) Ankyrin repeat proteins comprise a diverse family of bacterial type IV effectors. Science 320: 1651-4

Pearlman E, Jiwa AH, Engleberg NC, Eisenstein BI (1988) Growth of Legionella-Pneumophila in a Human Macrophage-Like (U937) Cell-Line. Microb Pathogenesis 5: 87-95

Pollard TD, Cooper JA (2009) Actin, a central player in cell shape and movement. Science 326: 1208-12

Prevention. CfDCa (2017) Annual Tables of Infectious Disease Data. . In Prevention CfDCa (ed)

Purcell M, Shuman HA (1998) The Legionella pneumophila icmGCDJBF genes are required for killing of human macrophages. Infect Immun 66: 2245-55

Qiu J, Luo ZQ (2017) Legionella and Coxiella effectors: strength in diversity and activity. Nat Rev Microbiol 15: 591-605

Qiu JZ, Sheedlo MJ, Yu KW, Tan YH, Nakayasu ES, Das C, Liu XY, Luo ZQ (2016) Ubiquitination independent of E1 and E2 enzymes by bacterial effectors. Nature 533: 120-+

Romano-Moreno M, Rojas AL, Williamson CD, Gershlick DC, Lucas M, Isupov MN, Bonifacino JS, Machner MP, Hierro A (2017) Molecular mechanism for the subversion of the retromer coat by the Legionella effector RidL. P Natl Acad Sci USA 114: E11151-E11160

Rotty JD, Wu C, Haynes EM, Suarez C, Winkelman JD, Johnson HE, Haugh JM, Kovar DR, Bear JE (2015) Profilin-1 serves as a gatekeeper for actin assembly by Arp2/3-dependent and -independent pathways. Dev Cell 32: 54-67

Roy CR, Berger KH, Isberg RR (1998) Legionella pneumophila DotA protein is required for early phagosome trafficking decisions that occur within minutes of bacterial uptake. Molecular Microbiology 28: 663-674

Sadosky AB, Wiater LA, Shuman HA (1993) Identification of Legionella pneumophila genes required for growth within and killing of human macrophages. Infect Immun 61: 5361-73

Schafer DA, Jennings PB, Cooper JA (1996) Dynamics of capping protein and actin assembly in vitro: uncapping barbed ends by polyphosphoinositides. J Cell Biol 135: 169-79

Schmidt G, Sehr P, Wilm M, Selzer J, Mann M, Aktories K (1997) Gln 63 of Rho is deamidated by Escherichia coli cytotoxic necrotizing factor-1. Nature 387: 725-9

Scott CC, Botelho RJ, Grinstein S (2003) Phagosome maturation: a few bugs in the system. J Membr Biol 193: 137-52

Segal G, Purcell M, Shuman HA (1998) Host cell killing and bacterial conjugation require overlapping sets of genes within a 22-kb region of the Legionella pneumophila genome. Proc Natl Acad Sci U S A 95: 1669-74

Segal G, Shuman HA (1997) Characterization of a new region required for macrophage killing by Legionella pneumophila. Infect Immun 65: 5057-66

Segal G, Shuman HA (1998) How is the intracellular fate of the Legionella pneumophila phagosome determined? Trends Microbiol 6: 253-255

Segal G, Shuman HA (1999) Possible origin of the Legionella pneumophila virulence genes and their relation to Coxiella burnetii. Molecular Microbiology 33: 669-670

Shao F, Merritt PM, Bao Z, Innes RW, Dixon JE (2002) A Yersinia effector and a Pseudomonas avirulence protein define a family of cysteine proteases functioning in bacterial pathogenesis. Cell 109: 575-88

Sheedlo MJ, Qiu JZ, Tan YH, Paul LN, Luo ZQ, Das C (2015) Structural basis of substrate recognition by a bacterial deubiquitinase important for dynamics of phagosome ubiquitination. P Natl Acad Sci USA 112: 15090-15095

Shen X, Banga S, Liu Y, Xu L, Gao P, Shamovsky I, Nudler E, Luo ZQ (2009) Targeting eEF1A by a Legionella pneumophila effector leads to inhibition of protein synthesis and induction of host stress response. Cell Microbiol 11: 911-26

Shi XQ, Halder P, Yavuz H, Jahn R, Shuman HA (2016) Direct targeting of membrane fusion by SNARE mimicry: Convergent evolution of Legionella effectors. P Natl Acad Sci USA 113: 8807-8812

Shohdy N, Efe JA, Emr SD, Shuman HA (2005) Pathogen effector protein screening in yeast identifies Legionella factors that interfere with membrane trafficking. P Natl Acad Sci USA 102: 4866-4871

Sigrist CJA, de Castro E, Cerutti L, Cuche BA, Hulo N, Bridge A, Bougueleret L, Xenarios I (2013) New and continuing developments at PROSITE. Nucleic Acids Res 41: E344-E347

Sohn YS, Shin HC, Park WS, Ge J, Kim CH, Lee BL, Heo WD, Jung JU, Rigden DJ, Oh BH (2015) Lpg0393 of Legionella pneumophila is a guanine-nucleotide exchange factor for Rab5, Rab21 and Rab22. Plos One 10: e0118683

Sturgill-Koszycki S, Swanson MS (2000) Legionella pneumophila replication vacuoles mature into acidic, endocytic organelles. Journal of Experimental Medicine 192: 1261-1272

Suarez C, Carroll RT, Burke TA, Christensen JR, Bestul AJ, Sees JA, James ML, Sirotkin V, Kovar DR (2015) Profilin Regulates F-Actin Network Homeostasis by Favoring Formin over Arp2/3 Complex. Dev Cell 32: 43-53

Swanson MS, Isberg RR (1995) Association of Legionella pneumophila with the macrophage endoplasmic reticulum. Infection and immunity 63: 3609-20

Tan Y, Arnold RJ, Luo ZQ (2011) Legionella pneumophila regulates the small GTPase Rab1 activity by reversible phosphorylcholination. Proc Natl Acad Sci U S A 108: 21212-7

Tan Y, Luo ZQ (2011a) Legionella pneumophila SidD is a deAMPylase that modifies Rab1. Nature 475: 506-9

Tan YH, Luo ZQ (2011b) Legionella pneumophila SidD is a deAMPylase that modifies Rab1. Nature 475: 506-U102

Tilney LG, Harb OS, Connelly PS, Robinson CG, Roy CR (2001) How the parasitic bacterium Legionella pneumophila modifies its phagosome and transforms it into rough ER: implications for conversion of plasma membrane to the ER membrane. J Cell Sci 114: 4637-50

Toulabi L, Wu XC, Cheng YS, Mao YX (2013) Identification and Structural Characterization of a Legionella Phosphoinositide Phosphatase. Journal of Biological Chemistry 288: 24518-24527

Viner R, Chetrit D, Ehrlich M, Segal G (2012) Identification of Two Legionella pneumophila Effectors that Manipulate Host Phospholipids Biosynthesis. Plos Pathogens 8

Vogel JP, Andrews HL, Wong SK, Isberg RR (1998) Conjugative transfer by the virulence system of Legionella pneumophila. Science 279: 873-6

Vogel JP, Roy C, Isberg RR (1996) Use of salt to isolate Legionella pneumophila mutants unable to replicate in macrophages. Ann N Y Acad Sci 797: 271-2

Weber S, Wagner M, Hilbi H (2014) Live-cell imaging of phosphoinositide dynamics and membrane architecture during Legionella infection. MBio 5: e00839-13

Weber SS, Ragaz C, Hilbi H (2009) The inositol polyphosphate 5-phosphatase OCRL1 restricts intracellular growth of Legionella, localizes to the replicative vacuole and binds to the bacterial effector LpnE. Cell Microbiol 11: 442-60

Weber SS, Ragaz C, Reus K, Nyfeler Y, Hilbi H (2006) Legionella pneumophila exploits PI(4)P to anchor secreted effector proteins to the replicative vacuole. PLoS Pathog 2: e46

Welch MD, Way M (2013) Arp2/3-Mediated Actin-Based Motility: A Tail of Pathogen Abuse. Cell Host & Microbe 14: 242-255

Wilkins BM, Thomas AT (2000) DNA-independent transport of plasmid primase protein between bacteria by the I1 conjugation system. Molecular Microbiology 38: 650-657

Worby CA, Mattoo S, Kruger RP, Corbeil LB, Koller A, Mendez JC, Zekarias B, Lazar C, Dixon JE (2009) The fic domain: regulation of cell signaling by adenylylation. Mol Cell 34: 93-103

Xu J, Xu D, Wan M, Yin L, Wang X, Wu L, Liu Y, Liu X, Zhou Y, Zhu Y (2017) Structural insights into the roles of the IcmS-IcmW complex in the type IVb secretion system of Legionella pneumophila. Proc Natl Acad Sci U S A 114: 13543-13548

Xu L, Luo ZQ (2013) Cell biology of infection by Legionella pneumophila. Microbes Infect 15: 157-67

Xu L, Shen X, Bryan A, Banga S, Swanson MS, Luo ZQ (2010a) Inhibition of host vacuolar H+-ATPase activity by a Legionella pneumophila effector. PLoS Pathog 6: e1000822

Xu L, Shen XH, Bryan A, Banga S, Swanson MS, Luo ZQ (2010b) Inhibition of Host Vacuolar H+-ATPase Activity by a Legionella pneumophila Effector. Plos Pathogens 6

Yao JL, Yang F, Sun XD, Wang S, Gan NH, Liu Q, Liu DD, Zhang X, Niu DW, Wei YQ, Ma C, Luo ZQ, Sun QX, Jia D (2018) Mechanism of inhibition of retromer transport by the bacterial effector RidL. P Natl Acad Sci USA 115: E1446-E1454

Yarbrough ML, Li Y, Kinch LN, Grishin NV, Ball HL, Orth K (2009) AMPylation of Rho GTPases by Vibrio VopS disrupts effector binding and downstream signaling. Science 323: 269-72

Zhu W, Banga S, Tan Y, Zheng C, Stephenson R, Gately J, Luo ZQ (2011a) Comprehensive identification of protein substrates of the Dot/Icm type IV transporter of Legionella pneumophila. Plos One 6: e17638

Zhu W, Luo ZQ (2013) Methods for determining protein translocation by the Legionella pneumophila Dot/Icm type IV secretion system. Methods Mol Biol 954: 323-32

Zhu WH, Banga S, Tan YH, Zheng C, Stephenson R, Gately J, Luo ZQ (2011b) Comprehensive Identification of Protein Substrates of the Dot/Icm Type IV Transporter of Legionella pneumophila. Plos One 6

Zhu WH, Hammad LA, Hsu FS, Mao YX, Luo ZQ (2013) Induction of caspase 3 activation by multiple Legionella pneumophila Dot/Icm substrates. Cellular Microbiology 15: 1783-1795

Zusman T, Aloni G, Halperin E, Kotzer H, Degtyar E, Feldman M, Segal G (2007) The response regulator PmrA is a major regulator of the icm/dot type IV secretion system in Legionella pneumophila and Coxiella burnetii. Molecular Microbiology 63: 1508-1523

Zusman T, Degtyar E, Segal G (2008) Identification of a hypervariable region containing new Legionella pneumophila Icm/Dot translocated substrates by using the conserved icmQ regulatory signature. Infection and Immunity 76: 4581-4591

# VITA

Yao Liu was born in Yangzhou, Jiangsu, China. He attended the Central South University (Changsha, China) in 2007 to study Biotechnology and obtained the Bachelor of Science degree in 2011. He joined Dr. Zhao-Qing Luo's Lab in 2013 and started his project on the modulation of actin cytoskeleton by *L. pneumophila* effectors. Later he identified that a *L. pneumophila* effector -RavK is able to disrupt actin cytoskeleton by cleaving actin. He will study *Mycobacterium tuberculosis* pathogenesis for his postdoctoral training in Dr. Sabine Ehrt's lab at Weill Cornell Medical College.

# PUBLICATIONS


1. Luo X, Wasilko DJ, **Liu Y**, Sun J, Wu X, Luo ZQ, Mao Y. Structure of the Legionella virulence factor, SidC reveals a unique PI (4) P-specific binding domain essential for its targeting to the bacterial phagosome. PLoS pathogens. 2015 Jun 12;11(6):e1004965.
2. **Liu Y**, Zhu W, Tan Y, Nakayasu ES, Staiger CJ, Luo ZQ. A Legionella effector disrupts host cytoskeletal structure by cleaving actin. PLoS pathogens. 2017 Jan 27;13(1):e1006186.
3. Zhao J, Beyrakhova K, **Liu Y**, Alvarez CP, Bueler SA, Xu L, Xu C, Boniecki MT, Kanelis V, Luo ZQ, Cygler M. Molecular basis for the binding and modulation of V-ATPase by a bacterial effector protein. PLoS pathogens. 2017 Jun 1;13(6):e1006394.
4. Qiu J, Yu K, Fei X, **Liu Y**, Nakayasu ES, Piehowski PD, Shaw JB, Puvar K, Das C, Liu X, Luo ZQ. A unique deubiquitinase that deconjugates phosphoribosyl-linked protein ubiquitination. Cell research. 2017 Jul;27(7):865.
5. Akturk A, Wasilko DJ, Wu X, **Liu Y**, Zhang Y, Qiu J, Luo ZQ, Reiter KH, Brzovic PS, Klevit RE, Mao Y. Mechanism of phosphoribosyl-ubiquitination mediated by a single Legionella effector. Nature. 2018 May 23:1.